

New active galactic nuclei detected in ROSAT All Sky Survey galaxies

II. The complete dataset^{*,**,***}

W. Kollatschny¹, R. Kotulla¹, W. Pietsch², K. Bischoff^{1,3}, M. Zetzl¹

¹ Institut für Astrophysik, Universität Göttingen, Friedrich-Hund Platz 1, D-37077 Göttingen, Germany
e-mail: wkollat@astro.physik.uni-goettingen.de

² Max-Planck-Institut für Extraterrestrische Physik, Giessenbachstrasse, D-85740 Garching, Germany

³ Halfmann Teleskoptechnik GmbH & Co. KG, Gessertshausener Str. 8, D-86356 Neusäß-Vogelsang, Germany

Received 2007; accepted 2008

ABSTRACT

Aims. The ROSAT ALL Sky Survey Bright Source Catalogue (RASS-BSC) has been correlated with the Catalogue of Principal Galaxies (PGC) to identify new extragalactic counterparts. 550 reliable optical counterparts have been detected. However there existed no optical spectra for about 200 Active Galactic Nuclei (AGN) candidates before the ROSAT ALL Sky Survey (RASS) was completed.

Methods. We took optical spectra of 176 X-ray candidates and companions at ESO, Calar Alto observatory and McDonald observatory. When necessary we used a line profile decomposition to measure line fluxes, widths and centers to classify their type of activity.

Results. We discuss the redshift-, linewidth-, as well as optical and X-ray luminosity distribution of our ROSAT selected sample. 139 galaxies of our 166 X-ray counterparts have been identified as AGN with 93 being Seyfert 1 galaxies (61%). Eighteen of them (20%) are Narrow Line Seyfert 1 galaxies. 34 X-ray candidates (21%) are LINERs and only eight candidates (5%) are Seyfert 2. The ratio of the number of Seyfert 1 galaxies to Seyfert 2 galaxies is about 11/1. Optical surveys result in ratios of 1/1.4. The high fraction of detected Seyfert 1 galaxies is explained by the sensitivity of the ROSAT to soft X-rays which are heavily absorbed in type 2 AGN. Two X-ray candidates are HII-galaxies and 25 candidates (15%) show no signs of spectral activity. The AGN in our RASS selected sample exhibit slightly higher optical luminosities ($M_B = (-20.71 \pm 1.75)$ mag) and similar X-ray luminosities ($\log(L_X[\text{erg s}^{-1}]) = 42.9 \pm 1.7$) compared to other AGN surveys. The $H\alpha$ line width distribution (FWHM) of our newly identified ROSAT AGN sample is similar to the line widths distribution based on SDSS AGN. However, our newly identified RASS AGN have rather reddish colors explaining why they have not been detected before in ultraviolet or blue excess surveys.

Key words. X-rays:galaxies – galaxies:active – surveys

1. Introduction

Canonical active galactic nuclei (AGN) are blue, UV-excess sources. They are known to be strong X-ray emitters (e.g. Fabbiano et al. 1992) in comparison to normal galaxies. However, not all AGN detected by their optical, infrared or radio properties have counterparts in X-ray surveys. The X-ray satellite ROSAT detected nearly 19 000 bright sources in the soft X-ray band (0.1-2.4 keV). These are listed in the ROSAT All Sky Survey Bright Source Catalogue (RASS-BSC) (Voges et al., 1993, 1999). We are interested in the optical spectral properties of ROSAT-selected AGN. On the one hand we wanted to take optical spectra of as many ROSAT counterparts as possible. On the other hand we wanted to test whether our newly identified RASS selected AGN show spectral properties different to those AGN that have been detected earlier with other strategies. A cor-

relation of the RASS with optical counterparts in the Principal Catalog of Galaxies (Paturel et al., 1989, 2003) resulted in about 900 extragalactic counterparts or candidates. These X-ray sources are mainly AGN or nearby galaxies. However, for about 200 AGN candidates no optical spectra existed when the ROSAT ALL Sky Survey (RASS) was completed.

This paper is the second in a series describing the optical spectra and the physical properties of these AGN. In the first paper the selection strategy was described by Pietsch et al. (1998 hereafter paper 1) and the optical spectra of 35 X-ray counterparts were presented.

In parallel to our new optical identifications we investigated X-ray and ROSAT-related AGN papers to determine whether some of our targets had been identified since (Moran et al. 1996, Simcoe et al. 1997 Bade et al., 1998, Motch et al. 1998, Appenzeller et al. 1998, Fischer et al. 1998, Bauer et al. 2000, Brinkmann et al. 2000, Vaughan et al. 2001 Xu et al., 2001, Grupe et al. 2004). Furthermore we checked SDSS-related papers (Adelman et al. 2006) as well as the Veron-Cetty catalogue of AGN (2006). In our list of 166 new AGN candidates we found some information with respect to 41 objects. In a preprint (Bischoff et al. 1999) we presented some preliminary data of 17 of our new AGN candidates.

* Based on observations collected at European Southern Observatory, Chile

** Based on observations taken at the German-Spanish Astronomical Center, Calar Alto, operated by the Max-Planck-Institute for Astronomy, Heidelberg jointly with the Spanish Commission for Astronomy.

*** Based on observations collected at McDonald Observatory

2. Observations

2.1. The ROSAT AGN sample

In paper 1 we described in detail our strategy to find new AGN in the ROSAT All Sky Survey. Further detailed information about the galaxy identification project can be found in Zimmermann et al. (2001). The selection is based on the empirical finding that most active galaxies are strong X-ray emitters in comparison to non-active galaxies. In the RASS-BSC (Voges 1999) nearly 19 000 X-ray sources are listed, having count rates in excess of 0.05 cts/s: These objects were subsequently cross-correlated with the Principal Catalog of Galaxies (Paturel et al. 1989, 2003). 904 X-ray sources were identified as having extragalactic counterparts.

Extended X-ray sources such as early-type galaxies or clusters of galaxies were rejected from our sample in the next step.

Finally, 547 correlations have been determined as reliable counterparts of compact extragalactic X-ray sources. These sources were cross-checked with the NASA Extragalactic Database (NED): 349 sources were known active galaxies. However, no spectral information existed for 198 AGN candidates. Our goal was to obtain spectra of as many of these objects as possible.

2.2. Optical observations

Table 2 contains information on our observed sample of 166 X-ray counterparts as well as some information on ten additional companions of these counterparts. Given are the ROSAT name (1), the optical positions derived from the Digitized Sky Survey (DSS) (2 and 3), the object name (4), the X-ray count rate (5), derived X-ray luminosity (6), the apparent (7) and absolute (8) B-band magnitudes (for details see paper 1).

Figure 1 shows the spatial distribution – in equatorial coordinates – of all AGN candidates for which we have acquired spectra. They are distributed homogeneously over the whole sky, except for the regions blocked by the Milky Way. The sky distribution of all 904 extragalactic X-ray counterparts has been shown by Zimmermann et al. (2001) (their Fig. 3).

We obtained optical spectra of our X-ray candidate galaxies during five observing campaigns. We used the 2.2 m telescope at Calar Alto Observatory in Spain, the 2.2 m telescope at La Silla/ESO in Chile, as well as the 2.7 m telescope at McDonald Observatory in Texas. We obtained spectra of 176 AGN candidates and companion galaxies. In a few cases we observed more than one object when there was more than one candidate in the ROSAT error box. We identified 166 AGN and non-AGN as optical counterparts of ROSAT RASS sources. Details of the observations, such as the observing periods, the telescopes and spectrographs we used, as well as the wavelength coverage of the spectra are listed in Table 1.

The observing dates of the individual galaxies and exposure times are listed in Table 3. Exposure times range from 10 to 45 minutes. The spectrograph slits had projected widths of 1.5 to 2 arc sec. We had typical seeing conditions of 1 to 1.5 arc sec. The slit was oriented in a north-south direction, in most cases, to minimize the impact of light losses caused by differential refraction.

Our spectra typically cover a wavelength range from 3800/4700 Å to 7300/8200 Å (see Table 1) with a spectral resolution of 8 to 10 Å. Additional spectra were taken after each object exposure for wavelength calibration. Various standard stars were observed for flux calibration.

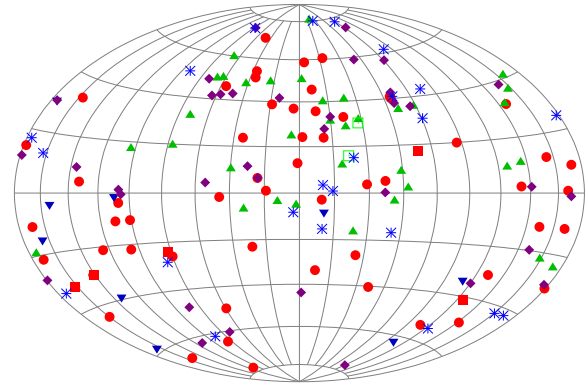


Fig. 1. Aitoff projection of all selected sources in J2000 equatorial coordinates (Center of the plot: RA=12h, DEC=0°; RA increases to the right.). There is a homogenous spatial distribution of our X-ray selected galaxies, except for the regions blocked by the Milky Way. The symbols used in this and all following plots: Sy 1 type objects: filled red circles, intermediate types (Sy 1.5/1.8/1.9): green upward triangles, Sy 2: blue downward triangles, LINERS: purple diamonds, H II: green open squares, non-active: blue stars.

Table 1. List of our observing runs giving the telescopes and instruments used for the acquisition of the spectra as well as their wavelength range.

#	Observing run	Telescope	Instrument (CCD)	$\lambda\lambda$ [Å]
1	96/11/02-06	ESO 2.2m ^a	EFOSC2 (LORAL)	3800–8000
2	97/07/02-06	ESO 2.2m ^a	EFOSC2 (LORAL)	4100–7400
3	97/07/28-08/01	CA 2.2m ^b	CAFOS (SITe#1d)	4200–8200
4	98/03/01-05	CA 2.2m ^b	CAFOS (SITe#1d)	4200–8200
5	00/02/08-09	MDO 2.7m ^c	LCS (TK3/CC1)	4700–7300

^a La Silla, Chile

^b Calar Alto, Spain

^c McDonald Observatory, Texas, USA

2.3. Data reduction

The reduction of the spectra (bias subtraction, cosmic ray correction, flat-field correction, 2D-wavelength calibration, night sky subtraction, flux calibration) was done in a homogeneous way with the IRAF reduction packages¹. We extracted spectra of the central 3 arc sec. The wavelength calibration was done using comparison spectra of He-Ar (runs #1, #2), Hg-Cd-He (#3, #4) and He-Ne (#5). The flux calibration was done by means of the standard stars HD 49798 (#1), NGC 7293 (#1), Turnshek et al. 1990), BD 332642 (#4) and BD G191B2B (#4,5).

Redshifts, emission line intensities and line widths were derived from individual emission/absorption lines as well as determined by fitting line complexes ($H\alpha$ narrow and broad, [N II], [S II]; $H\beta$ narrow and broad). Only the narrow Balmer line components were used for the diagnostic diagram (see Fig. 7) to derive their activity type.

¹ IRAF is distributed by the National Optical Astronomy Observatories, which are operated by the Association of Universities for Research in Astronomy, Inc., under cooperative agreement with the National Science Foundation.

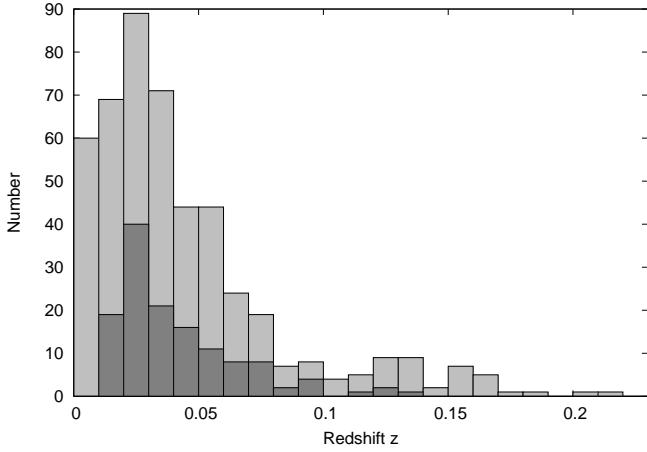


Fig. 2. Redshift distribution of our newly identified RASS AGN (dark columns). Two objects have redshifts of $z = 0.55$ and $z = 1.90$. The redshift distribution of the already known RASS AGN (Zimmermann et al. 2001) (grey columns) is shown for comparison.

3. Results

The optical spectra of the X-ray counterparts (AGN candidates) of our first observing run are published in Paper 1. All spectra taken during the remaining 4 observing runs are presented in Fig. 11.

We discriminated between the main X-ray counterpart and the galaxy companion when we observed more than one galaxy in the ROSAT error box.

The results derived from our optical spectroscopy are given in Table 3. We list the name of the object (1), the observing run (2), total exposure time used (3), observed redshift (4), flux ratios of $[\text{O III}]\lambda 5007/\text{H}\beta$ (5) and $[\text{N II}]\lambda 6583/\text{H}\alpha$ (6), Balmer decrement of the broad components (7), the width (FWHM) of the broad $\text{H}\alpha$ component (8) and the derived nuclear activity class (9). The galaxies already presented in paper 1 are marked [P1]. Those galaxies that since have been classified as an AGN are marked [V]. The detailed literature can be found in the Veron-Cetty Catalogue of AGN (2006).

3.1. Redshift distribution

The redshifts we derived from the object spectra are given in Table 3. The typical error is less than 160 km s^{-1} . There is no redshift information for the BL Lac candidates.

Figure 2 shows the redshift distribution of our newly identified RASS AGN (dark columns). Most objects have redshifts below $z = 0.1$. Two objects not shown in Fig. 2 have redshifts of $z = 0.55$ and $z = 1.90$. Our median redshift is $z = 0.0327$. The redshift distribution of the already known RASS AGN (Zimmermann et al. 2001) with a median redshift of $z = 0.0330$ is shown for comparison (grey columns). The median redshift of all RASS AGN also amounts to $z = 0.0330$.

These numbers can be compared with the SDSS redshift distribution of AGN found by Anderson et al. (2007). Limiting their X-ray count rate to sources in excess of 0.05 cts/s, they find a peak at $z \approx 0.15$. This shows that our ROSAT selected AGN are nearby objects compared to the Anderson sample.

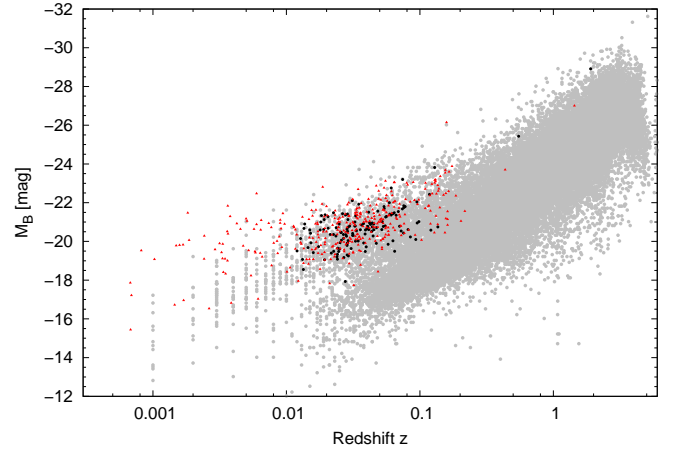


Fig. 3. M_B distribution of our newly identified RASS AGN (black dots) as a function of redshift as well as the M_B distribution of the already known RASS AGN (red dots). Grey points are objects from the 12th edition Quasar catalogue of Veron-Cetty (2006). We converted all magnitudes to a Hubble constant of $H_0 = 75 \text{ km s}^{-1} \text{ Mpc}^{-1}$.

3.2. Optical and X-ray luminosity distribution

The B-Band flux, the ROSAT soft (0.1 – 2.4 keV) X-ray flux as well as the luminosities of our sample galaxies are given in Table 2. A Hubble constant of $H_0 = 75 \text{ km s}^{-1} \text{ Mpc}^{-1}$ was used throughout this paper. For all objects with redshift information (all objects except those classified as BL Lac, see Table 3, cols 4 and 9) we calculated distances and luminosities. Four objects have absolute magnitudes $\leq -23 \text{ mag}$ classifying them as QSO.

The optical luminosity distribution of our sources is shown in Figs. 3 and 4. Optical magnitudes of our galaxies are taken from the PGC. We calculated in a homogeneous way the absolute M_B magnitudes of our sample galaxies with the formula given by Veron-Cetty (2006) to compare our magnitudes with the AGN magnitudes in their Quasar and AGN catalogue. Figure 3 shows the B-band magnitudes M_B of our newly identified RASS AGN (black dots) as a function of redshift, the M_B distribution of the already known RASS AGN (red dots) as well as the Seyfert magnitude distribution in the Veron-Cetty Catalogue. The grey points represent all Seyfert/LINER galaxies given in the Veron-Cetty Catalog (2006). The absolute magnitudes from the Veron-Cetty Catalogue have been transformed to a Hubble constant of $H_0 = 75 \text{ km s}^{-1} \text{ Mpc}^{-1}$.

The RASS selected AGN are located in optically bright galaxies compared to the AGN in the catalogue of Veron-Cetty (2006) (see Fig. 3). The mean absolute magnitude of our newly identified RASS AGN is $M_B = (-20.71 \pm 1.75) \text{ mag}$. This value is identical to the magnitude of the already known RASS AGN (Zimmermann et al. 2001)(see Fig. 4) and only slightly above the mean value $M_B = -20.46 \text{ mag}$ of Ho et al. (1997). Ho et al. (1997) derived their absolute magnitude from a sample of all nearby AGN. The optical brightness of our newly identified ROSAT AGN cannot be responsible for them remaining undetected so far.

To compute the soft X-ray (0.1 – 2.4 keV) energy fluxes from the ROSAT count rates we assumed a power-law spectrum

$$f_E dE \propto E^{-\Gamma+1} dE, \quad (1)$$

where $f_E dE$ is the energy flux between E and $E + dE$. The spectral index was fixed to $\Gamma = 2.3$, a typical value for galaxies ob-

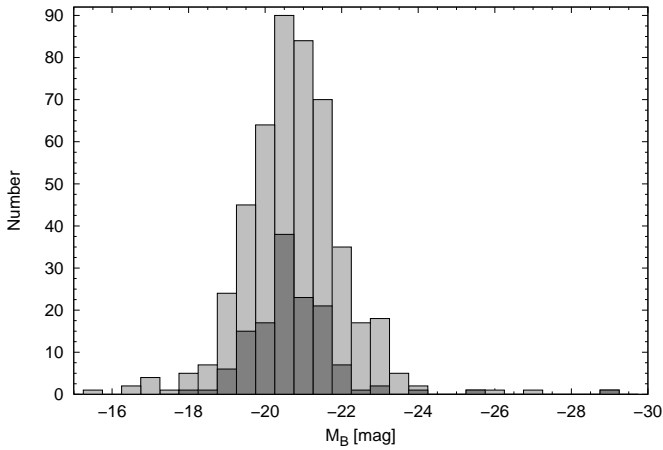


Fig. 4. M_B distribution of our newly identified RASS AGN (dark columns) as well as the M_B distribution of the already known RASS AGN (Zimmermann et al. 2001) (grey columns) shown for comparison.

served with ROSAT (Hasinger 1991, Boller 1998). We only consider the Galactic H_I -column density (Dickey 1990) along the line of sight as absorbing column density, so the given fluxes have to be understood as lower limits for the intrinsic fluxes emitted by the active nuclei from within its host galaxy.

In Fig. 5 we plot the X-ray luminosity of our newly identified RASS galaxies as a function of redshift z . Most objects lie one to two orders above the selection-limit of 0.05 cts/s indicated by the dotted line. The points below the selection limit are located at positions with a lower H_I column density than the mean and therefore have lower flux levels than expected for objects with an average column density.

The X-ray luminosity distribution L_X of our newly identified RASS AGN (dark columns) is shown in Fig. 6 together with the luminosity distribution L_X of the already known RASS AGN (Zimmermann et al. 2001) (grey columns). The distribution of both samples is best described by a Gaussian with FWHM = 1.66 dex around $\log(L_X[\text{erg s}^{-1}]) = 42.9$. Zimmermann et al. (2001) obtained X-ray luminosities of $\log(L_X) \approx 43.5 \pm 1.5$ for their sample of active galaxies and $\log(L_X) \approx 42.5 \pm 1.5$ for the candidate galaxies (their Fig. 9a). They rated those X-ray sources as candidate galaxies that were likely to possess hitherto unreported active galactic nuclei. The X-ray luminosity distribution of X-ray AGN selected from the SDSS (Anderson et al. 2003, 2007) and having redshifts $z \leq 0.15$ is shown for comparison. Their mean X-ray luminosity $\log(L_X) \approx 43.5 \pm 1.1$ is slightly above our value. However, they identified mostly quasars and Seyfert 1 galaxies in their sample.

3.3. AGN type distribution

To classify the activity type of our galaxies we measured the $H\alpha$, $H\beta$, $[O III]\lambda 5007$, and $[N II]\lambda 6583$ emission line intensities whenever it was possible. The broad Balmer lines were fitted with one or multiple line components. Table 3 lists the measured line ratio of the $[O III]\lambda 5007/H\beta$ and $[N II]\lambda 6583/H\alpha$ line ratios. We considered only the narrow Balmer line components for these line ratios.

The FWHM linewidth W_α of the broadest line component in the $H\alpha$ complex is given in Table 3 (column 8). The typical error

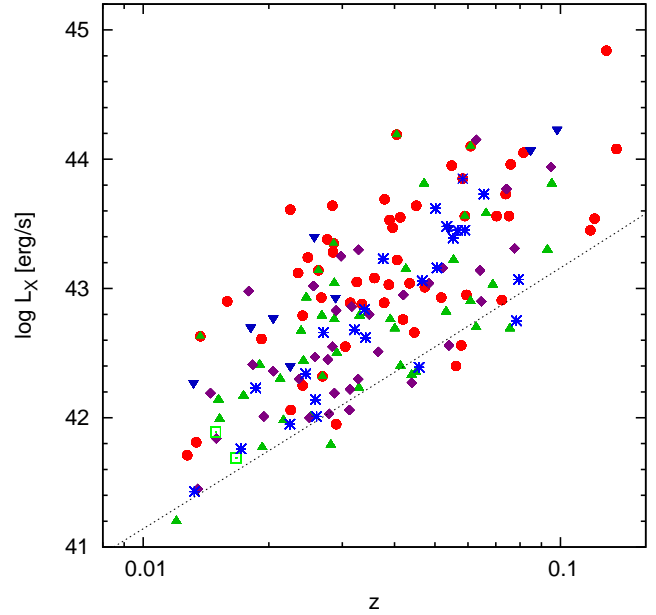


Fig. 5. X-ray luminosities as function of redshift z of our newly identified RASS galaxies. Symbol definition as in Fig. 1. The dashed line marks the detection limit of the RASS bright source catalog of 0.05 cts/s, converted to luminosities using the median galactic H_I column density of our sample ($0.258 \times 10^{21} \text{ cm}^{-2}$).

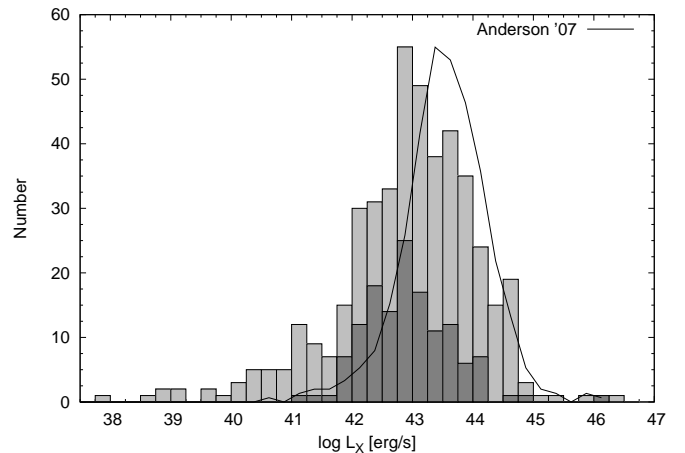


Fig. 6. Distribution of the X-ray luminosity L_X of our newly identified RASS AGN (dark columns) as well as the distribution of the already known RASS AGN (Zimmermann et al. 2001) (grey columns). Also shown for comparison is the relative distribution of Anderson et al. (2007) (solid line) for their X-ray AGN from the SDSS.

is 200 km s^{-1} . Column 7 gives the Balmer decrement $H\alpha/H\beta$ derived from the broad-line components only.

We classified our galaxies in the following way: Seyfert 1 type galaxies have single broad Balmer line components only in their spectra. Intermediate Seyfert types 1.5, 1.8 and 1.9 show broad as well as narrow Balmer line components; the intensity ratio of the broad Balmer line component decreases with respect to the narrow Balmer line component. We recalibrated all our galaxies in a homogeneous way - including those of Paper 1.

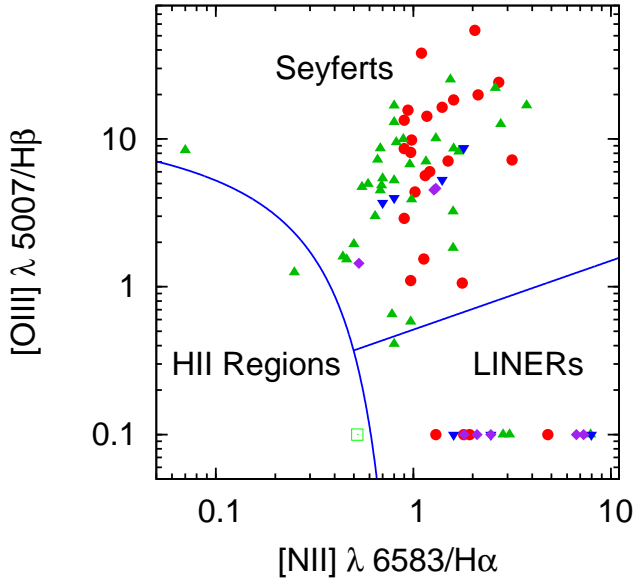


Fig. 7. Diagnostic Baldwin diagram of all our newly identified emission line galaxies with measured narrow components in all four lines. Also shown are the empirically determined dividing lines of Kewley et al. (2001) (solid line). Symbols are as described in Fig. 1.

In a few cases we made small changes in the classification of the intermediate type Seyferts. Narrow Line Seyfert 1 galaxies have single component Balmer lines with line widths of about less than 2500 km s^{-1} (Osterbrock 1985), only slightly broader than the forbidden narrow emission lines. Furthermore, these objects have relatively weak $[\text{O III}]\lambda 5007$ emission and strong FeII emission. Seyfert 2 galaxies, LINERs and HII galaxies show narrow emission lines only. On basis of their narrow line ratios $[\text{O III}]\lambda 5007/\text{H}\beta$ and $[\text{N II}]\lambda 6583/\text{H}\alpha$ we discriminate between Seyfert 2, LINER, and HII spectra (see Fig. 7). In Fig. 7 we show the dividing line for the different types (Kewley et al. 2001). In some LINERs we measured weak $[\text{N II}]$ and $\text{H}\alpha$ emission only, with upper limits for the $[\text{O III}]\lambda 5007$ line intensity. Here we set a value of 0.1 for the $[\text{O III}]\lambda 5007/\text{H}\beta$ intensity ratio.

BL Lac objects are characterized by their blue featureless continuum. Galaxies showing absorption line spectra only are classified as non-active galaxies.

Figure 8 shows the distribution of our newly identified RASS AGN and non-AGN types (dark columns) as well as the distribution of the already known RASS AGN (Zimmermann et al. 2001) (grey columns).

Only 27 galaxies (16.3%) of our 166 ROSAT selected galaxies show no nuclear activity: 2 HII-galaxies (1.2%) and 25 absorption line galaxies (15.1%). Some of the X-ray counterparts we classified as absorption line galaxies have very high X-ray luminosities (see Fig. 5). Seven of them show $\log(L_X) \geq 43.45$. It is not clear whether we took spectra of the wrong counterpart or whether these objects are highly obscured AGN. ROSAT could also have detected X-ray emission from an unknown galaxy group or cluster of which our candidate galaxy may be a member.

Most of our galaxies (60.8%) are of Seyfert type 1: 32 pure Seyfert 1 (19.3%), 43 intermediate Seyfert 1 (25.9%), and 18 NLS1 (10.8%). About one fifth of the Seyfert 1 galaxies are

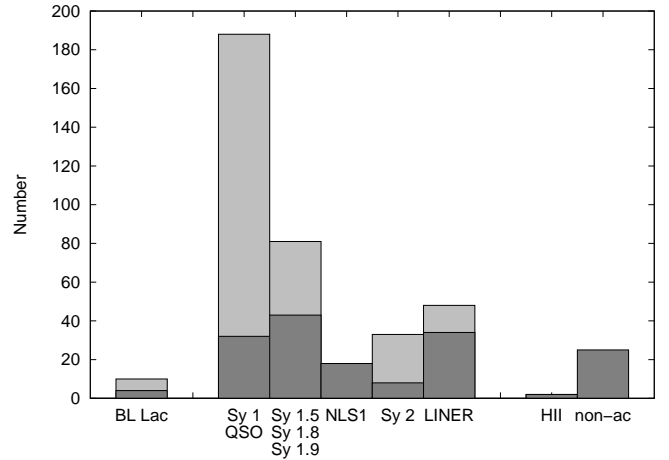


Fig. 8. Distribution of our newly identified RASS AGN and non-AGN types (dark columns) as well as the distribution of the already known RASS AGN (Zimmermann et al. 2001) (grey columns).

NLS1 galaxies. Among all Seyfert galaxies only 8 galaxies (4.8%) are of Seyfert type 2. Furthermore, we found 34 LINERs (20.5%) and 4 BL Lac objects (2.4%).

The AGN type distribution in our newly identified RASS AGN sample is similar to the distribution in the sample of Zimmermann et al. (2001) (see Fig. 8). However, the relative number of the pure Seyfert 1 types is greater in the sample of Zimmermann. On the other hand the relative number of intermediate Seyferts and LINERs is greater in our new RASS sample. This may be caused by the high quality of our spectra which allowed a more detailed classification.

3.4. Companion galaxies and galaxy pairs

The source of the X-ray emission could not always be identified with one optical galaxy only. In some cases we took more than one spectrum of objects within the X-ray error box.

We assigned that galaxy to the X-ray source that showed the highest activity degree in the optical spectrum. Data for the galaxies we identified as companion galaxies of the X-ray galaxies are given at the end of Table 2 and 3. MCG -01-22-27 is the companion of NGC 2617.

The X-ray quasar 1RXS J085001.4 + 701804 is an interesting object. This quasar shines through the outer disk of the spiral galaxy NGC 2650. We see absorption lines from the foreground galaxy in the quasar spectrum as a result of this projected superposition.

The rest of the new companion galaxies in our list are galaxy pairs.

3.5. Line width distribution

We derived $\text{H}\alpha$, $\text{H}\beta$, and $[\text{O III}]\lambda 5007$ line widths (FWHM) of all emission line galaxies of our new sample from single or multi-component fits. The spectral lines were adapted by single-component fits for starburst HII galaxies, LINERs, Seyfert 2 galaxies, Narrow-Line Seyfert 1 galaxies (NLS1), and pure Seyfert 1 galaxies. If the Balmer lines were fitted by more than one broad component and if the broadest component had a relative line intensity of at least 30 percent we present the line widths

(FWHM) of the broadest component in Table 3 (column 8) and Fig. 9.

We show the $H\alpha$ line width distribution (FWHM) of our AGN sample in Fig. 9. A step size of 1000 km s^{-1} was used. For comparison we also plot (solid line) the relative distribution of the $H\alpha$ line widths (FWHM) of Hao et al. (2005) who used a sample of AGN derived from the Sloan Digital Sky Survey (SDSS). The $H\alpha$ FWHM distribution of our ROSAT AGN sample resembles the $H\alpha$ FWHM distribution of the SDSS AGN sample.

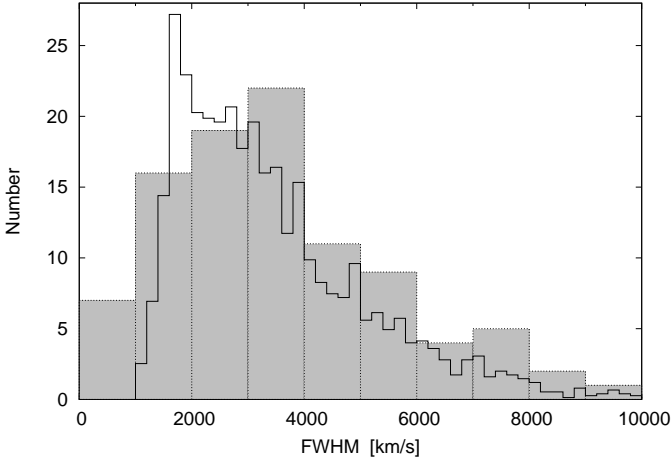


Fig. 9. $H\alpha$ line width distribution (FWHM) of our newly identified ROSAT AGN sample in steps of 1000 km s^{-1} . The solid line gives the scaled-down distribution of $H\alpha$ line widths of AGN derived from the Sloan Digital Sky Survey (Hao et al. 2005).

3.6. Optical to blue color distribution

Finally, we inspected the optical colors of our galaxy spectra to check whether the hitherto unknown ROSAT selected AGN have specific continuum properties. We derived B and V-band colors of our newly identified RASS-AGN with the IRAF task 'sbands'. Not all of our spectra cover the full wavelength range of the B-band filter. Therefore, we derived our B and V-band colors with a bandpass width of 200 \AA only for the sake of homogeneity. We compared these 'narrow-band' colors with 'full bandwidth' colors whenever we had the full wavelength range at our disposal. Furthermore, we compared our 'narrow-band' colors with data from the literature. They agree amongst each other within 0.1 mag .

We then compared the colors of our newly identified RASS AGN with an independent sample of all 764 AGN spectra derived from the Second Data Release of SDSS (Abazajian et al. 2004). These SDSS-AGN were selected by their classification as QSO in the SDSS database and limited to $z \leq 0.15$ to fit the redshift range of our sample. We determined the colors of these SDSS-AGN in the same way as explained above. The results are shown in Fig. 10.

The color distribution of the SDSS sample (black solid line) shows a Gaussian-like shape with a mean value of $(B - V) \approx 0.05 \text{ mag}$. The distribution of our newly identified RASS AGN contains far more red galaxies.

The shift of the $(B-V)$ distribution to the red by about 0.15 mag might be caused by the fact that the newly identified RASS AGN are systematically redder and/or that the relative number of

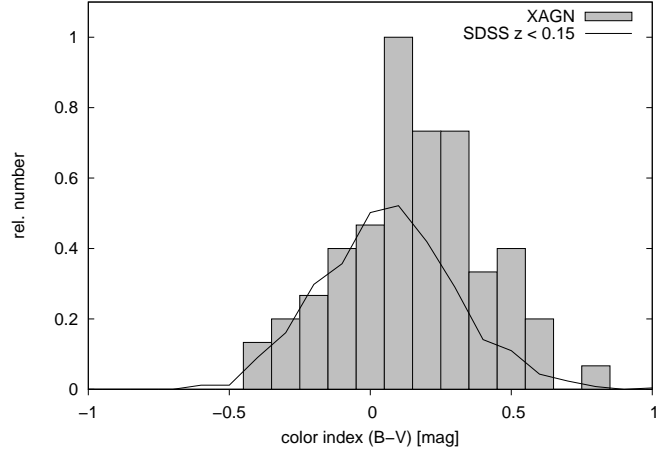


Fig. 10. Color distribution of our newly identified RASS AGN (shaded grey) and of a comparison sample consisting of all 764 $z \leq 0.15$ AGN from the Second Data Release of SDSS (black line).

intermediate Seyfert galaxies and LINERs is higher compared to optically selected AGN samples. Intermediate Seyfert galaxies and LINERs have redder colors than pure Sy 1 types. We derived the following colors from the spectra of our individual AGN types: Sy 1: $0.04 \pm 0.16 \text{ mag}$, Sy 1.5 - 1.9: $0.13 \pm 0.26 \text{ mag}$, NLS1: $-0.09 \pm 0.21 \text{ mag}$, Sy 2: $0.28 \pm 0.27 \text{ mag}$, LINER: $0.34 \pm 0.16 \text{ mag}$.

4. Discussion and conclusion

About 550 compact X-ray sources have been identified as AGN or AGN candidates by cross-correlating the ROSAT Bright Source Catalog with the Principal Catalog of Galaxies. 350 of these sources have been identified before as AGN on basis of their optical spectra. Cross-correlating the ROSAT Bright Source Catalog with the Principal Catalog of Galaxies yielded a sample of 198 galaxies with as yet unknown X-ray emission.

We took spectra of as many X-ray counterparts as possible in five optical spectroscopic campaigns. At the end we obtained spectra of 166 X-ray counterparts. Since the start of our identification campaign, 41 of these galaxies have likewise been identified as AGN by other observers (see introduction). Our AGN classification of the different types agrees with the classification of other authors - except for minor discrepancies in the subdivision. For homogeneity we used our spectra and classification schema for this investigation.

Most of our galaxies are nearby objects. We determined redshifts up to 0.15 with a median of $z = 0.033$. Only two AGN of our new sample are more distant objects (up to $z = 1.9$).

The RASS selected AGN show a mean absolute magnitude of $M_B = (-20.71 \pm 1.75) \text{ mag}$ in the optical. They are hosted by brighter galaxies compared to the AGN in the catalogue of Veron-Cetty (2006) (see Fig. 3). Ho et al. (1997) derived a mean magnitude of $M_B = -20.46 \text{ mag}$ from a sample of all nearby AGN. Therefore it is not due to their optical faintness that our ROSAT selected AGN have not been detected before.

Our X-ray luminosity distribution of the RASS selected AGN peaks at $\log(L_X[\text{erg s}^{-1}]) = 42.9 \pm 1.7$ (Fig. 6). This value should be compared with the peak in the luminosity $\log(L_X) \approx 43.5 \pm 1.1$ of X-ray AGN selected from the SDSS (Anderson et al. 2003, 2007) with redshifts below $z \leq 0.15$. They identified mostly quasars and Seyfert 1 galaxies in their sample which

might have caused the peak at slightly higher luminosities in the luminosity distribution.

We determined the activity type of our emission line galaxies on the basis of their Balmer line widths as well as narrow emission line ratios. 139 galaxies of our 166 ROSAT selected objects have been classified as AGN. This indicates that the X-ray selection criterion is very successful in finding new AGN. In the remaining 27 galaxies, faint AGN might still be buried that could not be separated in our spectra from the galaxy emission.

We compare the relative numbers of our Seyfert, LINER, H II and absorption line galaxies with the numbers derived from the Palomar Survey of all nearby galaxies (Ho et al. 1997). While the fraction of galaxies showing no sign of nuclear activity is the same in both samples (XAGN: 15.1% vs Ho: 13.6%) we find far more Seyfert type nuclei (XAGN: 60.8% vs Ho: 10.7%) in our ROSAT selected AGN. Contrary to this, H II galaxies are found in nearly half of all Palomar galaxies (Ho: 42.4% vs XAGN: 1.2%). The relative number of LINERs is higher in the Palomar Survey (XAGN: 20.5% vs Ho: 32.7%). This might be caused by the fact that it is more difficult to detect weak LINER properties in distant galaxies because of the lower S/N ratio.

The fraction of our new ROSAT-selected Seyfert 1 galaxies (pure Sy1, intermediate Sy1, and NLS1) is very high compared to type 2 Seyferts (see Fig. 8). The Seyfert 1/2 ratio is 11/1. This ratio is strongly affected by selection effects as ROSAT was most sensitive in the soft X-ray band which is heavily absorbed in type 2 AGN. Optical surveys do not suffer from this bias. Therefore, an Sy1/Sy2 ratio of 1:1.4 or an Sy 1 fraction of 42% as reported by Ho et al. (1997) may better reflect the true ratio.

We classified 18 galaxies as Narrow Line Seyfert 1 which is 20% of all broad-line AGN (Sy1 to Sy1.9). Other studies of RASS selected sources also detected many Narrow Line Seyfert 1 galaxies (e.g. Boller et al. 1996, Grupe et al. 1999). From NLS1 catalogs compiled from the SDSS AGN Catalog, Williams et al. (2002) found that roughly 15% of all broad line AGN are of NLS1-type, a number already suggested by Osterbrock (1987) and later confirmed by Zhou et al. (2007), who determined an average fraction of 14% (up to $\approx 20\%$ at $M_g \approx -22$ mag) for their sample of > 2000 NLS1-galaxies from SDSS-DR3.

The linewidth distribution of our ROSAT sample matches that of the SDSS AGN (Hao et al. 2005).

We also determined optical broad-band colors from the galaxy spectra. We found that our hitherto undetected ROSAT AGN have redder colors in comparison to an independent sample of AGN spectra derived from the Second Data Release of SDSS (Abazajian et al. 2004) (see Fig. 10).

The redder color of our newly identified RASS AGN might explain why they have not been detected in earlier AGN searches which concentrated on blue or UV-excess galaxies or on optical identifications based on low resolution objective prism spectra. All these surveys were not complete and were biased towards single broad band or spectral properties. That our galaxies predominantly are fainter in the blue might be caused by internal absorption of the central nonthermal radiation within the host galaxy. Another explanation could be that the redder distribution of our newly identified RASS AGN might be caused by the fact that the relative number of intermediate Seyfert galaxies and Liners in our sample is higher compared to other optically selected AGN samples. Intermediate Seyfert galaxies and Liners have redder colors than pure Sy 1 types.

In a future paper we will supplement our optical and X-ray data with data at radio and far-infrared wavelengths to further

constrain our classification and to gain a deeper insight into their X-ray production mechanisms.

Acknowledgements. The ROSAT project was supported by the German Bundesministerium für Bildung, Wissenschaft, Forschung und Technologie (BMBF/DARA) and by the Max Planck Gesellschaft (MPG). This work was partially supported by the *Deutsche Forschungsgemeinschaft*, DFG project number Ko 857 and the *Verbundforschung Astrophysik* (Grant 05 A5PD 1/4).

References

- Abazajian, K., Adelman-McCarthy, J. K., Agüeros, M. A., et al. 2004, *AJ*, 128, 502
- Adelman-McCarthy, J., Agüeros, M. A., Allam, S. S., et al. 2006, *ApJS* 162, 38
- Anderson, S. F., Margon, B., Voges, W et al. 2007, *AJ* 133, 313
- Anderson, S. F., Voges, W, Margon, B. et al. 2003, *AJ* 126, 2209
- Appenzeller, I., Thiering, I., Zickgraf F. J. et al. 1998, *ApJS* 117, 319
- Bade, N., Engels, D., Voges, W. et al. 1998, *A&AS* 127, 145
- Bauer, F. E., Condon, J. J., Thuan, T. X., & Broderick, J. J. 2000, *ApJS* 129, 547
- Bischoff, K., Pietsch W., Boller T. et al. 1999, *MPE Report* 272, 226
- Boller, T., Brandt, W. N. & Fink, H. 1996, *A&A* 305, 53
- Boller, T., Bertoldi, F., Dennefeld, M. & Voges, W 1998, *A&AS* 129, 87
- Brinkmann, W., Laurent-Muelheisen, S. A., Voges, W. et al. 2000, *A&A* 356,445.
- Dickey, J. M. & Lockman 1990, *ARA&A* 28, 215
- Fabbiano, G., Kim, G. W. & Trinchieri, G. 1992, *ApJS* 80, 531
- Fischer, J. U., Hasinger, G., Schwobe, A. D. et al. 1998, *AN* 319, 347.
- Grupe, D., Beuermann, K., Mannheim, K. & Thomas, H. C. 1999, *A&A* 350, 805
- Grupe, D., Wills, B. J., Leighly, K. M. & Meusinger, H. 2004, *AJ* 127, 156.
- Hao, L., Strauss, M. A.; Tremonti, C. A., et al. 2005, *AJ* 129, 1783
- Hasinger, G., Truemper, J. & Schmidt, M. 1991, *A&A* 246, L2
- Ho, L.C., Filippenko, A.V., Sargent, W. 1997, *ApJ* 487, 568
- Kewley, L. J., Dopita, M. A., Sutherland, R. S. et al. 2001, *ApJ* 556, 121
- Moran, E.C., Halpern, J.P., Helfand D.J. 1996, *ApJS* 106, 341
- Motch, C., Guillout, P., Haberl, F., et al. 1998, *A&AS* 132, 34
- Osterbrock, D. E. 1987, *Lecture Notes in Physics, Active Galactic Nuclei* (Springer, Heidelberg)
- Osterbrock, D. E., Pogge, R. W. 1985, *ApJ* 297, 166
- Paturel, G., Fouque, P., Bottinelli, L. & Gouguenheim, L. 1989, *A&AS* 80, 299
- Paturel, G., Petit, C., Prugniel, P., et al. 2003, *A&A* 412, 45
- Pietsch, W., Bischoff, K., Boller, T., et al. 1998, *A&A* 333, 48 (Paper 1)
- Simcoe, R., McLeod, K. K., Schachter, J., Elvis M. 1997, *ApJ* 489, 615
- Turnshek, D.A., Bohlin, R.J., Williamson, R.I. et al. 1990, *AJ* 99, 1243
- Vaughan, S., Edelson, R., Warwick, R. et al. 2001, *MNRAS* 327, 673.
- Veron-Cetty, M.P. & Veron, P. 2006, *VizieR Online Data Catalogue* 7248.0
- Voges, W. 1993, *AdSpR* 13, 391
- Voges, W., Aschenbach, B., Boller, et al. 1999, *A&A* 349, 389
- Williams, R. J., Pogge, R. W., & Mathur, S. 2002, *AJ* 124, 3042
- Xu, D. W., Wei J. Y., Hu, J. Y. 2001, *Chinese J. A&A* 1, 46
- Zhou, H., Wang, T., Yuan, W. et al. 2007, *ApJ* 658, L13
- Zimmermann, H.-U., Boller, T., Doebereiner, S., Pietsch, W. 2001, *A&A* 378, 30

Table 2. X-ray identification information

ROSAT-Name	RA, DEC (J2000.0)		Name	Count rate	$\log(L_X)$	m_B	M_B
(1)	[h m s]	[d m s]	(4)	[cts s ⁻¹]	[ergs ⁻¹]	[mag]	[mag]
(1)	(2)	(3)	(4)	(5)	(6)	(7)	(8)
IRXS J000156.7 – 273748	00 01 55.8	-27 37 38	ESO 409-003	0.067 ± 0.0171	42.55	14.66	-20.63
IRXS J000459.1 + 114205	00 04 58.4	11 42 03	UGC 32	0.148 ± 0.0205	43.77	14.20	-23.20
IRXS J000805.6 + 145027	00 08 05.6	14 50 23	CGCG 433-025	0.179 ± 0.0180	43.64	15.70	-20.60
IRXS J001530.2 + 172009	00 15 30.9	17 19 42	NGC 57	0.072 ± 0.0198	42.23	13.14	-21.23
IRXS J001823.8 + 300357	00 17 23.6	30 08 48	NGC 71	0.006 ± 0.0202	42.40	14.42	-20.36
IRXS J001823.8 + 300357	00 18 22.8	30 04 47	NGC 70	0.006 ± 0.0202	42.30	14.18	-20.71
IRXS J002108.1 – 190950	00 21 13.2	-19 10 44	PKS 0018-19	0.104 ± 0.0195	43.81	17.00	-20.95
IRXS J002534.9 – 330255	00 25 31.3	-33 02 48	ESO 350-015	0.249 ± 0.0310	43.62	14.23	-22.31
IRXS J003413.7 – 212619	00 34 13.5	-21 26 20	HCG 4a	0.330 ± 0.0350	43.14	13.70	-21.43
IRXS J004236.9 – 104919	00 42 36.7	-10 49 22	VIII Zw 36	0.244 ± 0.0280	43.55	14.60	-21.51
IRXS J010013.4 – 151755	01 00 15.9	-15 17 57	MCG -03-03-017	0.151 ± 0.0207	43.47	14.90	-21.80
IRXS J010517.5 – 582618	01 05 16.5	-58 26 13	ESO 113-010	0.182 ± 0.0390	43.40	14.60	-20.47
IRXS J010918.0 + 131011	01 09 18.4	13 10 08	UGC 716	0.069 ± 0.0150	43.45	15.60	-21.30
IRXS J011219.5 – 320338	01 12 19.2	-32 03 44	NGC 427	0.153 ± 0.0230	42.88	15.10	-20.55
IRXS J011233.3 – 320139	01 12 32.6	-32 01 44	RX J011232.8-320140	0.033 ± 0.0020		21.10	
IRXS J012018.8 – 440748	01 20 19.6	-44 07 43	ESO 244-017	0.305 ± 0.0310	43.12	14.60	-20.28
IRXS J013124.2 + 330837	01 31 23.8	33 08 38	KUG 0128+328	0.104 ± 0.0187	43.56	16.50	-20.78
IRXS J014526.6 – 034945	01 45 25.3	-03 49 39	MCG -01-05-031	0.175 ± 0.0290	42.70	13.30	-21.00
IRXS J014739.5 – 660952	01 47 39.5	-66 09 49	ESO 080-005	0.091 ± 0.0200	42.32	16.00	-19.17
IRXS J023513.9 – 293616	02 35 13.4	-29 36 18	ESO 416-002	0.356 ± 0.0340	43.56	14.90	-22.00
IRXS J023536.7 – 293845	02 35 36.6	-29 38 44	PHL 1389	0.043 ± 0.0040		16.10	
IRXS J025552.4 + 091853	02 55 52.2	09 18 42	IC 1867	0.083 ± 0.0190	43.02	14.60	-20.46
IRXS J030606.3 – 390212	03 06 05.9	-30 02 10	NGC 1217	0.193 ± 0.0230	42.77	13.30	-21.28
IRXS J030825.9 + 040637	03 08 26.3	04 06 40	NGC 1218	0.175 ± 0.0210	43.35	13.90	-21.41
IRXS J034203.8 – 211428	03 42 02.8	-21 14 26	ESO 548-081	0.258 ± 0.0260	42.63	12.80	-20.90
IRXS J042710.2 – 624712	04 27 12.5	-62 47 09	AM 0426-625	0.097 ± 0.0150	42.41	13.00	-21.33
IRXS J043520.2 – 780150	04 35 16.2	-78 01 57	ESO 015-011	0.274 ± 0.0250	44.10	14.20	-22.76
IRXS J043813.8 – 104740	04 38 13.8	-10 47 45	MCG -02-12-050	0.066 ± 0.0160	43.08	15.20	-20.60
IRXS J044148.1 – 011806	04 41 48.3	-01 18 10	UGC 3134	0.083 ± 0.0160	42.93	14.20	-21.13
IRXS J045142.3 – 034834	04 51 41.4	-03 48 34	MCG -01-13-025	0.281 ± 0.0290	42.90	14.60	-19.42
IRXS J045256.6 + 011854	04 52 58.9	01 19 53	UGC 3194	0.053 ± 0.0140	42.03	14.90	-20.35
IRXS J045840.4 – 215922	04 58 40.3	-21 59 32	ESO 552-039	0.106 ± 0.0180	43.47	16.30	-19.72
IRXS J045859.6 – 002904	04 58 54.6	-00 29 20	NGC 1713	0.120 ± 0.0199	41.84	13.30	-20.59
IRXS J050820.9 + 172134	05 08 20.5	17 21 58	CGCG 469-001	0.060 ± 0.0128	41.77	15.40	-19.05
IRXS J051621.5 – 103341	05 16 21.2	-10 33 40	MCG -02-14-009	0.307 ± 0.0290	43.64	15.50	-19.79
IRXS J054715.3 + 505209	05 47 14.9	50 52 15	UGC 3355	0.057 ± 0.0144	42.01	15.60	-19.50
IRXS J055559.4 – 612438	05 55 52.6	-61 24 14	ESO 120-023	0.093 ± 0.0070	43.23	15.30	-20.60
IRXS J060635.4 – 472957	06 06 35.8	-47 29 56	ESO 254-017	0.213 ± 0.0160	43.25	14.60	-20.79
IRXS J062122.8 – 280712	06 21 26.2	-28 06 53	ESO 425-019	0.077 ± 0.0129	41.95	13.40	-21.38
IRXS J062307.7 – 643618	06 23 07.7	-64 36 21	PMN J0623-6436	0.417 ± 0.0130	44.84	14.80	-23.82
IRXS J063059.7 – 240636	06 30 59.4	-24 06 46	PMN J0630-2406	0.084 ± 0.0140		15.40	
IRXS J064011.5 – 255337	06 40 11.8	-25 53 43	ESO 490-026	0.273 ± 0.0290	43.24	14.10	-20.90
IRXS J064710.4 + 741433	06 47 14.0	74 14 12	NGC 2256	0.078 ± 0.0148	41.76	14.00	-20.19
IRXS J064748.3 + 742850	06 47 45.8	74 28 54	NGC 2258	0.062 ± 0.0131	41.45	13.00	-20.67
IRXS J065214.0 + 193147	06 52 15.1	19 31 57	CGCG 085-010	0.080 ± 0.0153	42.90	15.60	-21.36
IRXS J070907.6 + 483657	07 09 08.0	49 36 56	NGC 2329	0.106 ± 0.0194	42.01	13.10	-21.37
IRXS J071148.0 + 321902	07 11 47.7	32 18 36	B2 0708+32b	0.332 ± 0.0293	43.58	15.80	-21.35
IRXS J071204.2 – 603005	07 12 03.3	-60 30 30	ESO 122-016 (NE)	0.106 ± 0.1000	43.30	14.60	-21.00
IRXS J073353.4 + 491737	07 33 53.1	49 17 31	UGC 3901	0.080 ± 0.0164	41.98	15.30	-19.40
IRXS J073727.1 + 594143	07 37 30.1	59 41 03	UGC 3927	0.062 ± 0.0177	42.40	15.50	-20.61
IRXS J074701.7 + 413211	07 47 02.0	41 32 10	UGC 4018	0.077 ± 0.0143	42.19	14.80	-20.52
IRXS J075151.6 + 494854	07 51 51.9	49 48 52	MCG +08-15-09	0.067 ± 0.0141	42.01	15.10	-19.93
IRXS J080157.7 – 494639	08 01 57.9	-49 46 42	ESO 209-012	0.163 ± 0.0160	44.19	15.30	-20.77
IRXS J081021.3 + 421657	08 10 23.3	42 16 26	CGCG 207-040	0.138 ± 0.0215	43.14	15.60	-21.48
IRXS J081517.8 + 460429	08 15 16.9	46 04 31	MCG +08-15-56	0.138 ± 0.0190	42.76	15.20	-20.95
IRXS J082321.4 + 042231	08 23 21.7	04 22 21	IC 505	0.095 ± 0.0231	42.30	14.80	-20.80
IRXS J083539.1 – 040508	08 35 38.8	-04 05 17	NGC 2617	0.193 ± 0.0313	41.99	14.00	-19.93
IRXS J084456.2 + 425826	08 44 56.6	42 58 35	MCG +07-18-43	0.064 ± 0.0134	42.56	15.00	-21.70
IRXS J085001.4 + 701804	08 50 02.3	70 18 06	QSO east of NGC 2650	0.057 ± 0.0144	46.01	16.00	-28.91
IRXS J085617.7 – 013809	08 56 17.8	-01 39 08	CGCG 005-037	0.128 ± 0.0219	42.95	15.50	-21.41
IRXS J091345.4 + 474208	09 13 45.4	47 42 06	MCG +08-17-60	0.148 ± 0.0212	42.82	15.90	-20.77
IRXS J092115.9 + 101747	09 21 15.5	10 17 41	VIII Zw 45	0.141 ± 0.0296	42.69	15.40	-20.65
IRXS J093308.2 + 534754	09 33 08.9	53 47 49	KUG 0929+540	0.067 ± 0.0181	42.56	17.00	-19.85
IRXS J093642.6 + 505249	09 36 43.1	50 52 49	KUG 0933+511	0.054 ± 0.0133	42.40	15.50	-21.29

Table 2. (continued)

ROSAT-Name	RA, DEC (J2000.0)		Name	Count rate	$\log(L_X)$	m_B	M_B
(1)	[h m s]	[d m s]	(4)	[cts s ⁻¹]	[ergs ⁻¹]	[mag]	[mag]
	(2)	(3)		(5)	(6)	(7)	(8)
IRXS J094204.0 + 234106	09 42 04.8	23 41 07	CGCG 122-055	0.120 ± 0.0181	42.06	15.30	-19.49
IRXS J095154.9 - 064916	09 51 55.0	-06 49 23	NGC 3035	0.263 ± 0.0274	42.14	13.50	-20.42
IRXS J095948.0 + 112926	09 59 46.8	11 28 20	CGCG 064-024	0.159 ± 0.0238	43.31	15.70	-21.80
IRXS J100554.9 - 230318	10 05 55.4	-23 03 25	ESO 499-041	0.131 ± 0.0188	41.71	13.40	-20.15
IRXS J102403.1 + 062954	10 23 59.8	06 29 08	CGCG 037-022	0.119 ± 0.0198	42.66	16.00	-20.28
IRXS J102445.5 + 062455	10 24 43.5	06 26 03	CGCG 037-028	0.052 ± 0.0141	42.27	15.50	-20.75
IRXS J102841.7 + 490425	10 28 42.0	49 04 19	CGCG 240-047	0.073 ± 0.0138	42.33	15.30	-20.95
IRXS J104333.4 + 010109	10 43 32.9	01 01 09	GNB 069	0.070 ± 0.0183	42.91	16.80	-20.54
IRXS J104439.4 + 384541	10 44 39.2	38 45 34	CGCG 212-045	0.351 ± 0.0303	42.89	15.00	-20.92
IRXS J110312.1 + 414200	11 03 11.0	41 42 19	MCG +07-23-15	0.117 ± 0.0216	42.22	15.10	-20.41
IRXS J110941.7 - 033915	11 09 42.9	-03 49 03	CGCG 011-012	0.161 ± 0.0243	42.76	15.40	-20.59
IRXS J114014.0 + 244150	11 40 13.9	24 41 49	NGC 3798	0.065 ± 0.0137	41.20	13.90	-19.51
IRXS J114429.9 + 365314	11 44 29.9	36 53 08	KUG 1141+371	1.368 ± 0.0740	43.53	16.50	-19.48
IRXS J114604.3 - 081550	11 49 03.8	-08 16 04	IC 734	0.080 ± 0.0183	43.07	16.00	-21.55
IRXS J115238.2 - 051229	11 52 36.2	-05 12 25	MCG -01-30-041	0.108 ± 0.0190	42.41	13.80	-20.62
IRXS J115537.0 + 125251	11 55 35.2	12 52 19	VIII Zw 153	0.134 ± 0.0291	43.54	17.90	-20.58
IRXS J120452.8 - 434353	12 04 52.9	-43 43 54	ESO 267-013	0.110 ± 0.0279	42.19	14.15	-19.68
IRXS J120655.0 + 501744	12 06 55.6	50 17 37	MCG +08-22-71	0.074 ± 0.0160	42.70	17.00	-20.03
IRXS J120719.4 + 241204	12 07 19.8	24 11 56	Mrk 648	0.196 ± 0.0235	42.93	16.00	-20.61
IRXS J121754.7 + 583936	12 17 55.0	58 39 35	Mrk 202	0.213 ± 0.0246	42.25	15.60	-19.33
IRXS J123651.1 + 453907	12 36 51.2	45 39 04	MCG +08-23-67	0.526 ± 0.0356	42.89	15.20	-20.31
IRXS J124046.8 - 333408	12 40 47.0	-33 34 12	ESO 381-007	0.446 ± 0.0455	43.95	15.94	-20.80
IRXS J124306.5 + 353859	12 43 07.4	35 39 05	KUG 1240+359	0.088 ± 0.0158	44.68	16.50	-25.43
IRXS J125042.5 - 024929	12 50 42.4	-02 49 31	CGCG 015-026	0.068 ± 0.0164	43.01	15.70	-20.71
IRXS J125253.5 - 152445	12 52 52.6	-15 24 48	NGC 4756	0.068 ± 0.0185	41.43	13.00	-20.63
IRXS J125347.3 + 032620	12 53 47.0	03 26 30	CGCG 043-056	0.186 ± 0.0422	43.73	15.70	-21.42
IRXS J125609.5 - 080906	12 56 10.1	-08 09 05	MCG -01-33-054	0.164 ± 0.0259	42.27	14.54	-19.07
IRXS J125851.4 + 235532	12 58 51.5	23 55 26	KUG 1256+241	0.430 ± 0.0319	43.56	17.00	-20.43
IRXS J130158.9 + 274708	13 02 00.1	27 46 58	CGCG 160-104	0.124 ± 0.0195	42.00	15.40	-19.61
IRXS J130456.7 + 395537	13 04 57.0	39 55 30	IC 4165	0.054 ± 0.0119	41.79	15.00	-20.27
IRXS J131633.1 + 005249	13 16 27.0	00 51 12	VIII Zw 272	0.053 ± 0.0159	42.75	17.30	-20.18
IRXS J131905.8 + 310854	13 19 06.0	31 08 53	CGCG 160-193	0.113 ± 0.0180	42.23	15.60	-20.01
IRXS J132016.3 + 308828	13 20 14.6	33 08 40	NGC 5098 (W)	0.180 ± 0.0214	42.51	15.00	-20.85
IRXS J133151.1 + 603451	13 31 50.7	60 34 48	MCG +10-19-84	0.125 ± 0.0156	43.45	16.00	-22.43
IRXS J133908.5 + 115855	13 39 08.5	11 58 54	VIII Zw 327	0.133 ± 0.0227	43.30	17.80	-20.10
IRXS J134352.7 + 803544	13 43 54.5	80 35 58	CGCG 365-016	0.050 ± 0.0098	42.35	15.40	-20.90
IRXS J135420.2 + 325547	13 53 20.0	32 55 48	UGC 8829	0.835 ± 0.0459	42.93	14.80	-20.36
IRXS J135536.3 + 155755	13 55 37.0	15 58 14	CGCG 103-009	0.112 ± 0.0206	41.69	15.70	-18.43
IRXS J135625.3 + 283138	13 56 25.3	28 31 35	MCG +05-33-24a	0.059 ± 0.0147	42.69	15.60	-21.84
IRXS J140543.6 + 405115	14 05 44.4	40 51 16	CGCG 219-050	0.164 ± 0.0207	43.03	15.70	-21.54
IRXS J140619.7 - 163721	14 06 20.7	-16 37 00	NPM1G -16.0443	0.057 ± 0.0155	42.50	16.09	-19.25
IRXS J140723.3 + 150447	14 07 22.3	15 04 39	CGCG 103-073	0.139 ± 0.0232	42.14	14.60	-20.49
IRXS J141802.6 + 800710	14 17 49.0	80 06 54	CGCG 353-034	0.057 ± 0.0107	42.39	15.30	-21.04
IRXS J141922.5 - 263842	14 19 22.4	-26 38 41	ESO 511-030	1.221 ± 0.0858	43.61	13.30	-21.48
IRXS J142916.8 + 300520	14 29 11.7	30 04 38	MCG +05-34-053	0.052 ± 0.0132	41.89	15.50	-18.38
IRXS J143207.9 + 313504	14 32 09.0	31 35 05	CGCG 163-074	0.079 ± 0.0154	43.22	15.50	-21.26
IRXS J143450.7 + 033834	14 34 50.6	03 38 43	CGCG 047-107	0.056 ± 0.0164	41.95	15.30	-20.04
IRXS J151447.8 - 402157	15 14 47.2	-40 21 35	ESO 328-036-S	0.162 ± 0.0236	42.79	15.85	-19.08
IRXS J151639.8 + 001454	15 16 40.2	00 15 02	CGCG 021-063	0.078 ± 0.0190	43.16	15.60	-21.02
IRXS J151750.8 + 050615	15 17 51.7	05 06 28	CGCG 049-106	0.107 ± 0.0194	43.03	15.60	-20.38
IRXS J153210.0 + 585434	15 32 16.1	58 54 04	VII Zw 608	0.028 ± 0.0086	42.90	17.60	-19.49
IRXS J153723.0 - 163551	15 37 22.4	-16 35 45	NGC 5959	0.054 ± 0.0139	42.34	14.50	-20.47
IRXS J153845.4 - 032309	15 38 44.7	-03 22 48	CGCG 022-021	0.070 ± 0.0149	42.44	15.29	-19.65
IRXS J155625.4 + 090311	15 56 25.9	09 03 19	Mrk 863	0.115 ± 0.0169	43.15	15.30	-20.88
IRXS J161040.5 + 020626	16 10 40.6	02 06 39	CGCG 023-021	0.105 ± 0.0169	42.76	15.40	-19.91
IRXS J161951.7 + 405834	16 19 51.3	40 58 47	KUG 1618+410	0.510 ± 0.0289	43.69	16.00	-19.92
IRXS J162013.1 + 400858	16 20 12.8	40 09 06	KUG 1618+402	0.356 ± 0.0239	43.28	16.00	-19.30
IRXS J162302.0 + 375506	16 23 03.1	37 55 21	NGC 6137	0.087 ± 0.0142	42.06	13.40	-22.10
IRXS J162637.1 + 350239	16 26 36.4	35 02 42	CGCG 196-064	0.081 ± 0.0128	42.81	15.70	-20.02
IRXS J162724.3 + 424041	16 27 25.2	42 40 47	NGC 6159	0.108 ± 0.0135	42.86	15.20	-20.32
IRXS J162741.8 + 405536	16 27 41.1	40 55 37	NGC 6160	0.069 ± 0.0122	42.68	14.20	-21.36
IRXS J170328.3 + 360400	17 03 27.8	36 04 20	MCG +06-37-023	0.520 ± 0.0095	44.15	15.60	-21.43
IRXS J171227.2 + 355256	17 12 28.4	35 53 03	MCG +06-38-005	0.125 ± 0.0139	42.79	15.00	-20.16
IRXS J171821.4 + 780118	17 18 16.6	78 01 05	MCG +13-12-022	0.126 ± 0.0102	43.45	15.30	-21.51
IRXS J172215.7 + 304250	17 22 15.4	30 42 40	MCG +05-41-010	0.077 ± 0.0137	43.06	15.60	-20.78

Table 2. (continued)

ROSAT-Name	RA, DEC (J2000.0)		Name	Count rate	$\log(L_X)$	m_B	M_B
(1)	[h m s]	[d m s]	(4)	[cts s ⁻¹]	[ergs ⁻¹]	[mag]	[mag]
(1)	(2)	(3)	(4)	(5)	(6)	(7)	(8)
IRXS J172324.0 + 565840	17 23 25.2	56 58 28	NGC 6370	0.054 ± 0.0079	42.45	13.88	-21.36
IRXS J173030.1 + 742244	17 30 36.9	74 22 34	NGC 6414	0.072 ± 0.0070	42.95	15.40	-20.75
IRXS J180242.4 + 424734	18 02 39.8	42 47 46	MCG +07-37-018 (NE)	0.082 ± 0.0114	43.16	14.40	-22.16
IRXS J180634.6 + 613554	18 06 35.6	61 35 38	MCG +10-26-015	0.091 ± 0.0054	42.66	16.20	-18.98
IRXS J182715.1 + 195624	18 27 14.8	19 56 19	MCG +03-47-002	0.129 ± 0.0179	43.22	15.30	-20.77
IRXS J184038.1 - 770930	18 40 38.5	-77 09 29	ESO 045-011	0.449 ± 0.0508	42.98	13.70	-20.59
IRXS J190937.0 - 622853	19 09 33.3	-62 28 40	ESO 104-041	0.241 ± 0.0467	44.07	17.46	-20.23
IRXS J192700.9 - 534241	19 27 01.6	-53 42 52	ESO 184-068	0.309 ± 0.0811	43.85	15.99	-20.88
IRXS J193139.0 - 335426	19 31 38.6	-33 54 43	PKS 1928-34	0.254 ± 0.0290	44.23	17.00	-21.02
IRXS J200052.6 - 343808	20 00 46.6	-34 38 00	ESO 399-015	0.066 ± 0.1920	42.47	15.02	-20.06
IRXS J200606.1 - 542212	20 09 06.4	-54 22 48	SGC 2005.13-5431.6	0.157 ± 0.0313	43.48	14.20	-22.47
IRXS J201731.2 - 411452	20 17 31.2	-41 14 52	RXS J201731.2-411452	0.145 ± 0.0390		17.00	
IRXS J202304.1 + 093233	20 23 04.3	09 32 38	CGCG 399-005	0.123 ± 0.0167	42.67	15.70	-19.21
IRXS J203433.1 - 303731	20 34 31.4	-30 37 29	IRAS F20315-3047	0.167 ± 0.0351	42.61	13.30	-21.13
IRXS J205522.8 + 022118	20 55 22.3	02 21 16	CGCG 374-029	0.055 ± 0.0118	41.81	15.10	-18.55
IRXS J210221.7 + 105812	21 02 21.6	10 58 16	CGCG 425-034	0.203 ± 0.0211	43.04	15.40	-19.91
IRXS J212324.3 + 021137	21 23 24.3	02 11 32	CGCG 375-033	0.071 ± 0.0156	43.04	14.90	-21.56
IRXS J212541.2 - 490935	21 25 40.7	-49 09 38	Fairall 969	0.145 ± 0.0237	43.73	15.71	-21.68
IRXS J213833.0 + 320507	21 39 33.4	32 05 06	CGCG 493-002	0.185 ± 0.0217	42.93	15.50	-19.48
IRXS J214153.6 + 315135	21 41 53.5	31 51 28	CGCG 493-004	0.074 ± 0.0149	43.04	15.70	-20.52
IRXS J215213.9 - 194256	21 52 09.6	-19 43 24	ESO 600-014	0.141 ± 0.0359	43.94	15.90	-22.04
IRXS J215656.8 - 113920	21 56 56.5	-11 39 32	NGC 7158	0.285 ± 0.0310	43.38	17.30	-17.93
IRXS J221231.8 + 384049	22 12 31.6	38 40 58	UGC 11950	0.072 ± 0.0123	42.36	13.90	-20.68
IRXS J221918.8 + 120757	22 19 18.5	12 07 53	II Zw 177	0.247 ± 0.0316	44.05	17.00	-20.61
IRXS J222706.1 + 362140	22 27 05.8	36 21 42	UGC 12040	0.058 ± 0.0113	42.30	14.30	-20.36
IRXS J223656.5 - 221321	22 36 55.9	-22 13 12	ESO 602-031	0.422 ± 0.0430	42.79	14.30	-21.32
IRXS J224156.7 - 423550	22 41 52.8	-42 35 35	ESO 290-003 (NE)	0.090 ± 0.0225	42.84	15.64	-20.04
IRXS J225850.4 + 405610	22 58 55.5	40 55 53	UGC 12282	0.065 ± 0.0128	42.17	14.49	-19.73
IRXS J230921.5 + 004540	23 09 20.3	00 45 23	IC 5287	0.091 ± 0.0180	43.05	14.80	-20.79
IRXS J231357.7 - 113027	23 13 57.0	-11 30 19	MCG -02-59-006	0.177 ± 0.0260	43.96	15.70	-21.75
IRXS J231853.1 - 010338	23 18 53.7	-01 03 38	UGC 12492	0.069 ± 0.0170	42.83	14.60	-20.74
IRXS J231906.5 - 420653	23 19 06.7	-42 05 37	MCG -07-47-032	0.120 ± 0.0329	43.39	15.00	-21.75
IRXS J232856.8 + 085346	23 28 58.5	08 54 39	MCG +01-59-085	0.092 ± 0.0155	44.08	18.00	-20.75
IRXS J233355.5 - 234336	23 33 55.2	-23 43 41	PKS 2331-240	0.437 ± 0.0387	43.81	16.50	-19.90
IRXS J234547.5 - 293053	23 45 47.6	-29 31 04	NGC 7749	0.079 ± 0.0187	42.80	13.82	-21.92
IRXS J235038.6 + 243321	23 50 36.6	24 33 22	UGC 12804	0.051 ± 0.0127	42.62	15.11	-20.58
IRXS J235728.4 - 302739	23 57 27.3	-30 27 37	AM 2354-304-E	0.057 ± 0.0447	42.55	15.82	-19.63
Companion galaxies, galaxy pairs							
IRXS J023513.9 - 293616	02 34 54.5	-29 34 28	RX J023454.8-293425	0.006 ± 0.0020	45.00	17.90	-24.53
IRXS J043520.2 - 780150	04 35 16.2	-78 01 57	ESO 015-011 (b)	0.077 ± 0.004		14.20	-22.78
IRXS J071204.2 - 603005	07 12 03.2	-60 30 30	ESO 122-016 (SW)	±		14.60	-20.99
IRXS J083539.1 - 040508	08 35 48.6	-04 05 33	MCG -01-22-27	±		15.00	-18.93
IRXS J085001.4 + 701804	08 49 58.4	70 17 58	NGC 2650	±		14.30	-19.53
IRXS J091345.4 + 474208	09 13 44.7	47 42 18	MCG +08-17-60 (N)	±		15.70	-20.97
IRXS J102403.1 + 062954	10 23 59.8	06 29 08	CGCG 037-023	±		15.60	-20.84
IRXS J132016.3 + 330828	13 20 17.5	33 08 45	NGC 5098 (E)	±		15.50	-20.35
IRXS J153210.0 + 585434	15 32 09.4	58 54 20	VII Zw 608 (W)	±		16.10	-17.13
IRXS J180242.4 + 424734	18 02 39.4	42 47 18	MCG +07-37-018 (SW)	±		15.40	-20.99

Table 3. Optical line properties

Name	Obs.Run	Exp. [s]	cz [km s ⁻¹]	[O III]/H β	[N II]/H α	H α /H β	FWHM _{Hα,br} [km s ⁻¹]	AGN type
(1)	(2)	(3)	(4)	(5)	(6)	(7)	(8)	(9)
ESO 409-003	97/07	1200	8520	4.52	1.27			LINER
UGC 32	97/08	1200	22260	0.10	2.47			LINER
CGCG 433-025 [P1]	96/11	1800	13520	38.00		2.29	8250	Sy 1
NGC 57	97/08	600	5580					non-ac
NGC 71	97/08	960	6750	0.10	7.97			Sy 2
NGC 70	97/08	960	7080	0.10	7.28			LINER
PKS 0018-19	97/07	2100	28590	25.22	1.54		8160	Sy 1.9
ESO 350-015	97/07	600	15060					non-ac
HCG 4a [P1]	96/11	900	7900	8.20	1.70		2100	Sy 1.9
VIII Zw 36 [P1]	96/11	900	12390	13.40	0.90	3.62	1950	Sy 1
MCG -03-03-017	97/07	600	16170	0.10	2.47			Sy 2
ESO 113-010 [P1]	96/11	900	7705	5.30	1.40		2000	Sy 2
UGC 716 [P1]	96/11	900	17710					non-ac
NGC 427 [P1]	96/11	2700	10035	0.10	1.80		5500	Sy 1
RX J011232.8-320140 [P1]	96/11	900						BL Lac
ESO 244-017 [P1]	96/11	900	7045	7.10	1.50	2.20	3000	Sy 1
KUG 0128+328	97/08	900	21090	54.28	2.05	4.96	2710	Sy 1
MCG -01-05-031 [P1]	96/11	900	5420	3.70	0.70			Sy 2
ESO 080-005 [P1]	96/11	1800	8080	13.00	0.80		3450	Sy 1.8
ESO 416-002 [P1]	96/11	1500	17710	22.10	2.60		16000	Sy 1.9
PHL 1389 [P1]	96/11	1200						BL Lac
IC 1867 [P1]	96/11	600	7680	0.10	6.70			LINER
NGC 1217 [P1]	96/11	600	6155					Sy 2
NGC 1218 [P1]	96/11	1500	8590	0.10	21.50		2950	Sy 1.9
ESO 548-081 [P1]	96/11	1500	4110	0.10	7.90		4450	Sy 1.9
AM 0426-625 [P1]	96/11	600	5490					LINER
ESO 015-011 [P1]	96/11	900	18280	5.40	0.70	1.99	2750	Sy 1.8
MCG -02-12-050 [P1]	96/11	1800	10730	38.10	1.10	2.52	5400	Sy 1
UGC 3134 [P1]	96/11	900	8665	4.00	0.80			Sy 2
MCG -01-13-025 [P1]	96/11	1200	4765	2.90	0.90	3.92	4500	Sy 1
UGC 3194	00/02	1800	8364		0.42		650	LINER
ESO 552-039 [P1]	96/11	1500	11870	18.40	1.60	2.22	4000	Sy 1
NGC 1713	98/03	1200	4491					LINER
CGCG 469-001 [V]	98/03	1200	5787	9.48	0.82	36.92	6460	Sy 1.9
MCG -02-14-009 [P1]	96/11	900	8530	8.60	0.90	2.86	2850	Sy 1
UGC 3355	98/03	600	7810					non-ac
ESO 120-023 [P1]	96/11	600	11280					non-ac
ESO 254-017 [P1]	96/11	1500	8925	0.10	2.10			LINER
ESO 425-019	00/02	1200	6740					non-ac
PMN J0623-6436 [P1]	96/11	1200	38640			2.72	2500	Sy 1
PMN J0630-2406 [P1]	96/11	600						BL Lac
ESO 490-026 [P1]	96/11	900	7450	16.40	1.40	2.14	4100	Sy 1
NGC 2256	98/03	1200	5145					non-ac
NGC 2258	98/03	1200	4060					LINER
CGCG 085-010	98/03	1200	18256	4.73	0.55	2.68	2060	Sy 1.5
NGC 2329	98/03	1200	5838					LINER
B2 0708+32b [V]	98/03	1500	19890	1.83	1.59	9.28	3880	Sy 1.9
ESO 122-016 (NE) [P1]	96/11	1200	9770					LINER
UGC 3901	98/03	1200	6508	0.65	0.78	6.43	9150	Sy 1.9
UGC 3927 [V]	98/03	1200	12405		4.98		3850	Sy 1.9
UGC 4018	00/02	1200	8616					LINER
MCG +08-15-09 [V]	98/03	1200	7556	7.23	0.66	19.37	4970	Sy 1.9
ESO 209-012 [P1]	96/11	1200	12140	8.60	1.60	2.93	3400	Sy 1.5
CGCG 207-040	00/02	1200	19249					LINER
MGC +08-15-56 [V]	98/03	1200	12583	3.97	0.94	6.07	1570	NLS1
IC 505	98/03	900	9821				300:	LINER
NGC 2617 [V]	98/03	1200	4575	7.03	1.16	21.86	7408	Sy 1.5
MCG +07-18-43	98/03	1200	16202		2.16		300:	LINER
QSO east of NGC 2650	98/03	420	(z=1.90)					QSO
CGCG 005-037 [V]	00/02	1500	17843	1.76	0.27	2.66	1440	NLS1
MCG +08-17-60 [V]	98/03	1200	15953	8.40	0.07	10.18	3350	Sy 1.5
VIII Zw 45 [V]	98/03	1200	12029	4.95	0.59	4.33	3480	Sy 1.5
KUG 0929+540	98/03	1200	17340	0.94	0.06	2.07	1760	NLS1
KUG 0933+511 [V]	98/03	600	16854	0.72	0.33	3.88	1820	NLS1

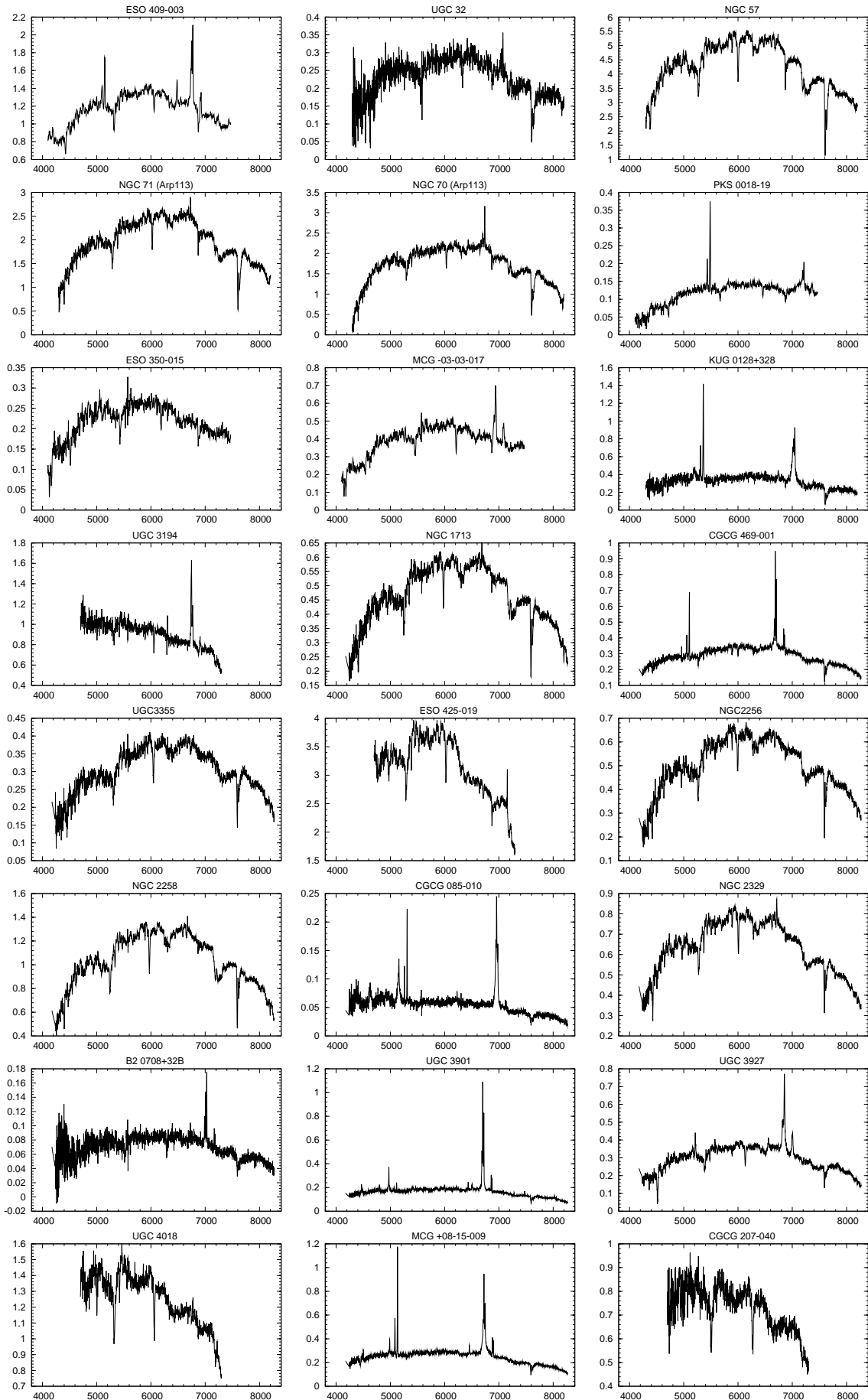
Table 3. (continued)

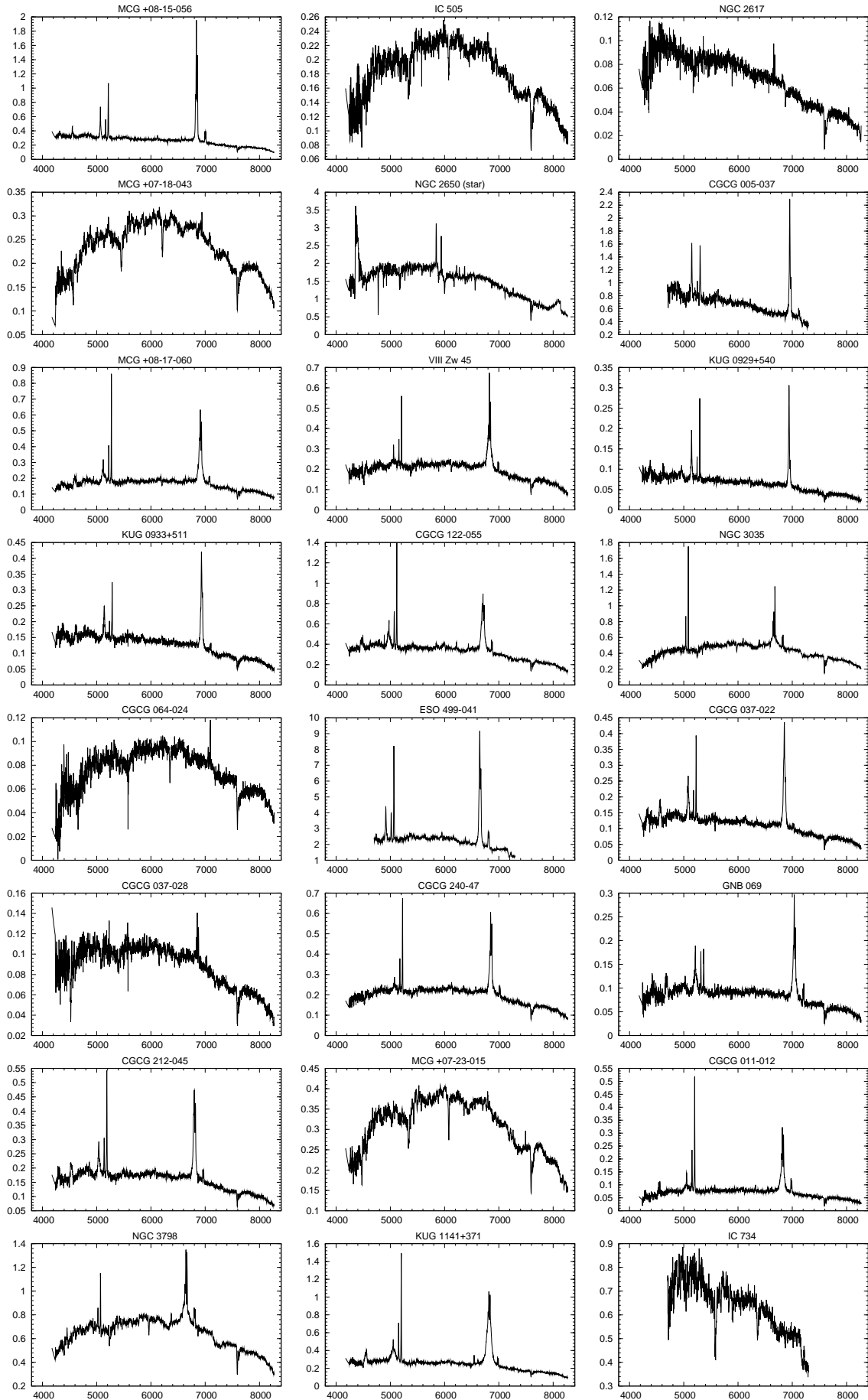
Name	Obs.Run	Exp. [s]	cz [km s ⁻¹]	[O III]/H β	[N II]/H α	H α /H β	FWHM _{Hα,br} [km s ⁻¹]	AGN type
(1)	(2)	(3)	(4)	(5)	(6)	(7)	(8)	(9)
CGCG 122-055	98/03	1200	6769	14.25	1.17	3.05	3120	Sy 1
NGC 3035 [V]	98/03	1200	4546		1.92		7460	Sy 1.8
CGCG 064-024	98/03	1200	23276		4.64		400:	LINER
ESO 499-041	00/02	1200	3826	1.80	0.58	5.26	1510	NLS1
CGCG 037-022	98/03	1200	13388	17.50	0.23	3.06	1940	NLS1
CGCG 037-028	98/03	1200	13204		0.82		500:	LINER
CGCG 240-047	98/03	1200	13191	16.83	0.80	7.52	2720	Sy 1.5
GNB 069 [V]	98/03	1200	21690	1.54	1.13	1.99	3670	Sy 1
CGCG 212-045 [V]	98/03	1200	11339	1.10	0.97		3250	Sy 1
MCG +07-23-15	98/03	1200	9394					LINER
CGCG 011-012	98/03	1200	11724	9.96	0.89	6.80	3710	Sy 1.5
NGC 3798 [V]	98/03	1200	3603	0.41	0.80	6.36	7990	Sy 1.5
KUG 1141+371 [V]	98/03	1200	11686	15.65	0.94	6.29	15310	Sy 1
IC 734	00/02	1800	23801					non-ac
MCG -01-30-041 [V]	97/07	1200	5700	3.00	0.64	2.66	5790	Sy 1.8
VIII Zw 153 [V]	98/03	1200	36201		0.19	2.23	4750	Sy 1
ESO 267-013	97/07	1200	4350	1.44	0.53			LINER
MCG +08-22-71	98/03	1200	18841	4.48	0.68	4.37	2370	Sy 1.8
Mrk 648	98/03	1200	15534	0.69	0.00	3.84	2690	NLS1
Mrk 202 [V]	98/03	1200	7234	3.15	0.37	2.87	2360	NLS1
MCG +08-23-67 [V]	98/03	1200	9398	10.34	0.85	5.61	1510	NLS1
ESO 381-007 [V]	97/07	1200	16470	9.85	0.98	3.50	4710	Sy 1
KUG 1240+359 [V]	98/03	1800	164591	0.40				QSO
CGCG 015-026 [V]	97/07	1800	14190	19.86	2.13	2.80	5620	Sy 1
NGC 4756	00/02	1200	3981					non-ac
CGCG 043-056	97/07	600	19650					non-ac
MCG -01-33-054	97/07	1200	3960	0.10	1.60			Sy 2
KUG 1256+241 [V]	00/02	1800	22586	8.12	0.97	1.87	5130	Sy 1
CGCG 160-104 [V]	98/03	1200	7506	-0.54	-1.58		690	LINER
IC 4165 [V]	98/03	2400	8447		1.02		3810	Sy 1.9
VIII Zw 272	98/03	600	23513					non-ac
CGCG 160-193 [V]	98/03	1200	9870	0.58	0.97	1.91	3270	Sy 1.5
NGC 5098	98/03	600	10970		3.76		500:	LINER
MCG +10-19-84 [V]	98/03	2400	35364	1.06	1.77	5.01	5610	Sy 1
VIII Zw 327	98/03	1200	27898	3.51				Sy 1.5
CGCG 365-016	00/02	1200	13519	3.23	1.59	3.32	1100	Sy 1.9
UGC 8829 [V]	98/03	1200	8015	5.66	1.15	9.35	19710	Sy 1
CGCG 103-009	98/03	1200	5000		0.35		230	H II
MCG +05-33-24a [V]	98/03	1200	22705	1.53	0.46	3.89	1770	Sy 1.8
CGCG 219-050	98/03	1500	20656		2.92		7570	Sy 1.5
NPM1G -16.0443	97/07	1200	8730	5.24	0.80	6.16	2400	Sy 1.5
CGCG 103-073	98/03	600	7758					non-ac
CGCG 353-034	98/03	600	13747					non-ac
ESO 511-030 [V]	97/07	600	6750	24.22	2.71	3.10	3620	Sy 1
MCG +05-34-053	97/08	600	4470	0.10	0.52			H II
CGCG 163-074	97/08	1200	16620	8.64	0.68	2.80	3590	Sy 1.5
CGCG 047-107 [V]	98/03	2700	8696	9.06	0.41	5.32	1320	NLS1
ESO 328-036-S	97/07	1200	7230	0.10	1.93	2.86	3750	Sy 1
CGCG 021-063 [V]	97/07	1800	15660	4.64	1.30		3640	LINER
CGCG 049-106	97/07	1200	11640	14.43	1.64	4.65	2190	NLS1
VII Zw 608	97/08	1200	19380	0.10	1.81			LINER
NGC 5959	97/07	600	7350					non-ac
CGCG 022-021 [V]	97/07	1200	7260	3.90	0.98		4310	Sy 1.8
Mrk 863 [V]	97/07	600	12780	1.94	0.50	2.80	2760	Sy 1.5
CGCG 023-021	97/07	1800	8610	0.10	3.07		4090	Sy 1.9
KUG 1618+410 [V]	97/08	1200	11370	14.64	0.27	2.78	2150	NLS1
KUG 1618+402 [V]	97/08	1200	8550	16.16	0.27	3.76	2160	NLS1
NGC 6137	98/03	600	9356		1.03		1440	LINER
CGCG 196-064	97/08	1200	10350	1.25	0.25	4.06	1650	Sy 1.9
NGC 6159	97/08	600	9480					LINER
NGC 6160	97/08	600	9630					non-ac
MCG +06-37-023	97/08	600	18840					LINER
MCG +06-38-005	97/08	1200	8040	6.72	0.96	2.97	7450	Sy 1.5
MCG +13-12-022	97/08	900	17010					non-ac
MCG +05-41-010	97/08	600	13980					non-ac

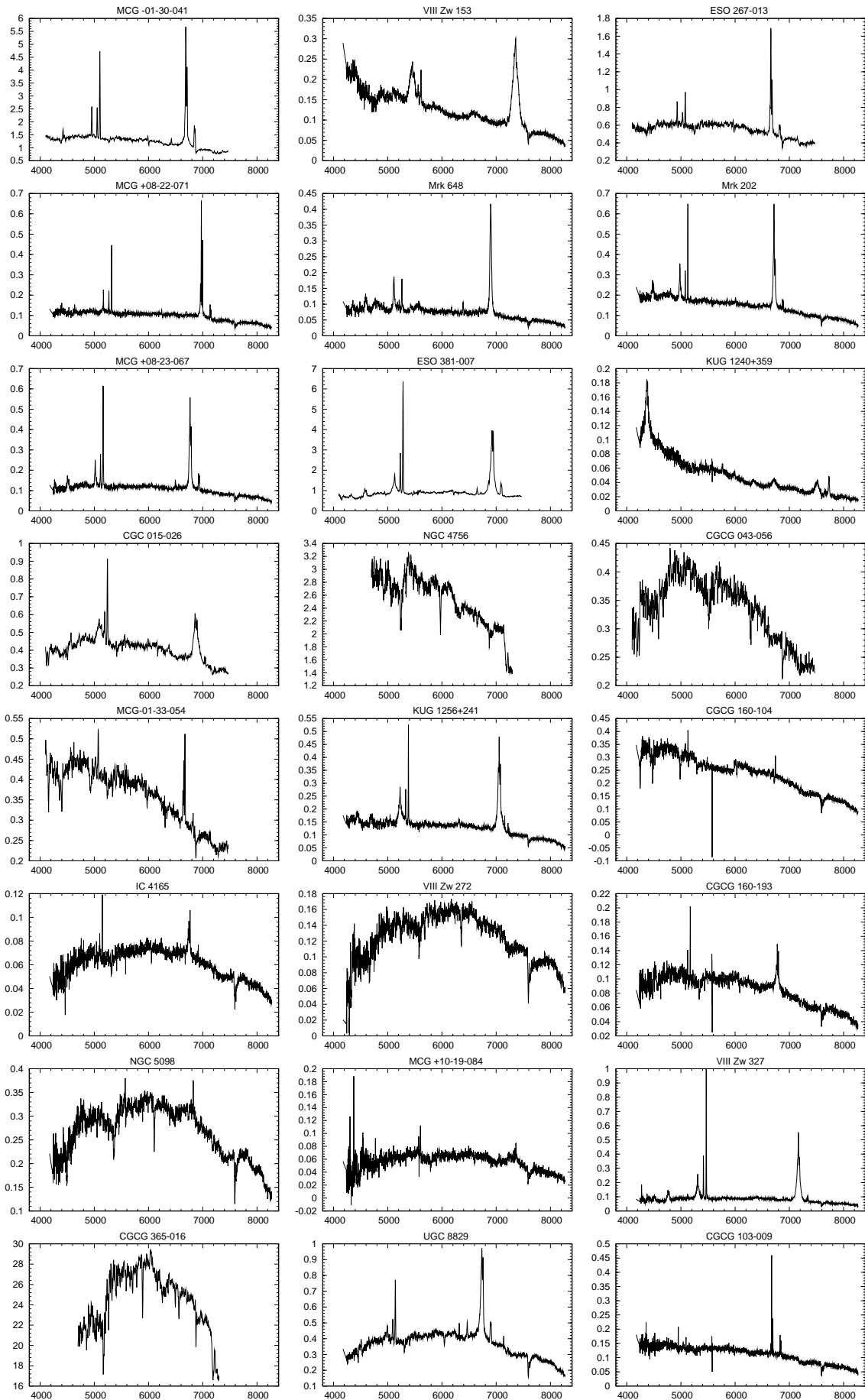
Table 3. (continued)

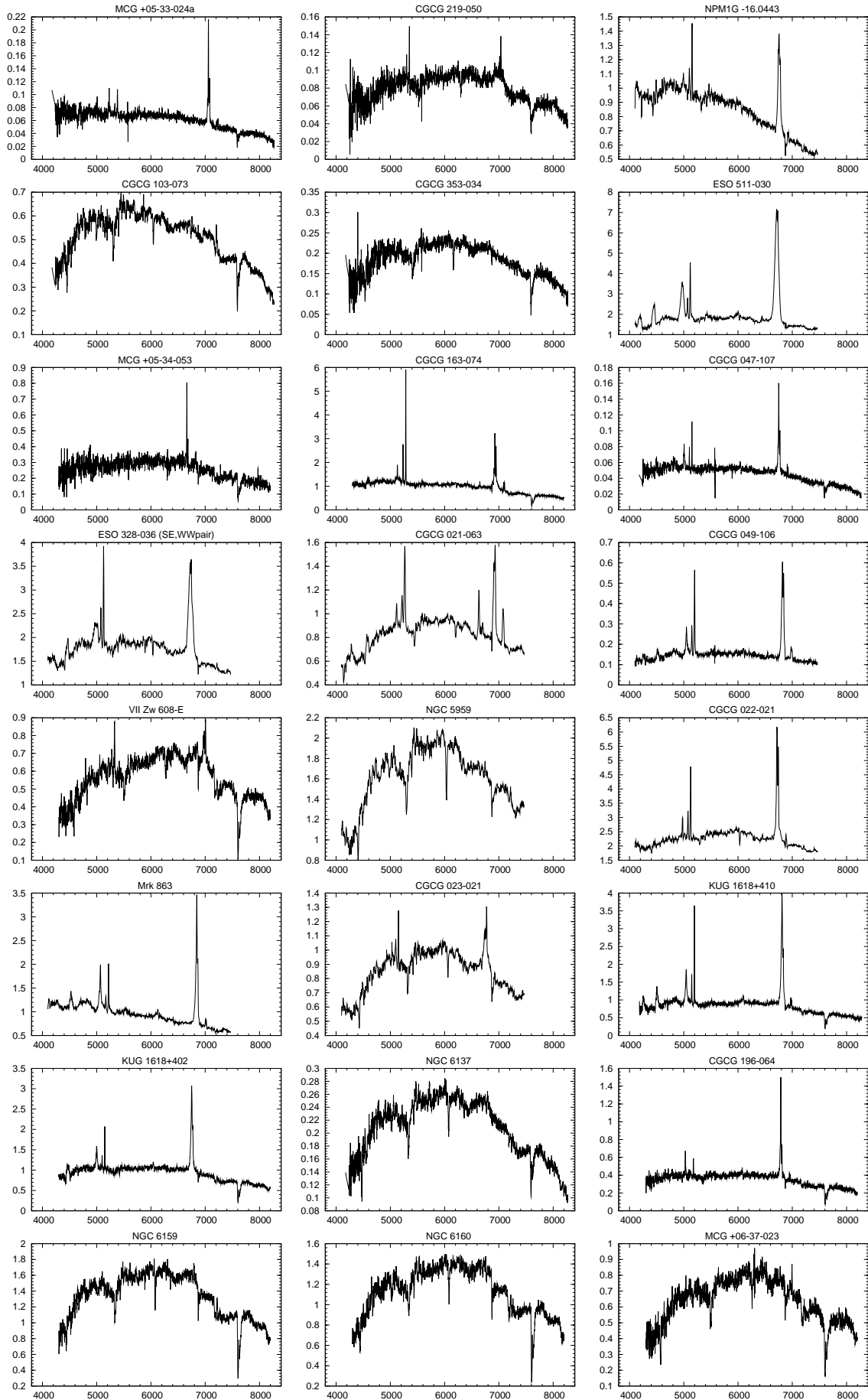
Name	Obs.Run	Exp. [s]	cz [km s ⁻¹]	[O III]/H β	[N II]/H α	H α /H β	FWHM _{Hα,br} [km s ⁻¹]	AGN type
(1)	(2)	(3)	(4)	(5)	(6)	(7)	(8)	(9)
NGC 6370	97/08	600	8310					LINER
NGC 6414	97/08	1800	12600					non-ac
MCG +07-37-018 (NE)	97/08	600	15180					non-ac
MCG +10-26-015	97/08	600	8100					non-ac
MCG +03-47-002	97/08	1200	12180	4.38	1.02	2.80	3930	Sy 1
ESO 045-011	97/07	1800	5370					LINER
ESO 104-041 (A)	97/07	1200	25440			2.86	6980	Sy 1
ESO 184-068	97/07	600	17490					non-ac
PKS 1928-34	97/07	1800	29460	8.70	1.80			Sy 2
ESO 399-015	97/07	1200	7740					LINER
SGC 2005.13-5431.6	97/07	600	16020					non-ac
RXS J201731.2-411452	97/07	900						BL Lac
CGCG 399-005	97/07	1200	7170	12.61	2.77		6790	Sy 1.9
IRAS F20315-3047 [V]	97/07	1800	5760	6.02	1.21	2.92	3320	Sy 1
CGCG 374-029	97/07	1200	4020	36.07	1.62	5.37	2040	NLS1
CGCG 425-034 [V]	97/07	2400	8610	1.60	0.44	2.80	6460	Sy 1.5
CGCG 375-033	97/07	600	14520					LINER
Fairall 969	97/07	3600	22170	7.22	3.16	2.80	3660	Sy 1
CGCG 493-002	97/08	1200	7380	4.84	0.69		5220	Sy 1.8
CGCG 493-004	97/08	1200	13050	0.41	0.04	2.84	1410	NLS1
ESO 600-014	97/07	600	28470					LINER
NGC 7158 [P1]	96/11	900	8275	10.90	0.90		2100	NLS1
UGC 11950	97/08	600	6150					LINER
II Zw 177 [V]	97/07	1800	24450	10.55	1.28	2.66	1180	NLS1
UGC 12040	97/08	1800	6390	0.10	2.85		4020	Sy 1.9
ESO 602-031 [P1]	96/11	1800	9895	10.10	1.30		5900	Sy 1.8
ESO 290-003 (NE)	97/07	1200	10170					non-ac
UGC 12282	97/08	1200	5220	16.85	3.75		5660	Sy 1.9
IC 5287 [P1]	96/11	1800	9750	0.10	4.80	3.30	4200	Sy 1
MCG -02-59-006 [P1]	96/11	900	22790	0.10	1.30		3700	Sy 1
UGC 12492 [P1]	96/11	600	8710					LINER
MCG -07-47-032	97/07	600	16590					non-ac
MCG +01-59-085	97/07	1500	40860					Sy 1
PKS 2331-240 [V]	97/07	1800	14130	6.86			3700	Sy 1.9
NGC 7749	97/07	600	10440					LINER
UGC 12804	97/08	600	10230					non-ac
AM 2354-304-E [V]	97/07	1200	9150	0.10		2.80	1970	NLS1
Companion galaxies, galaxy pairs								
RX J023454.8-293425 [P1]	96/11	3000	203550					QSO
ESO 015-011 (b) [P1]	96/11	900	18430	1.40	0.90			LINER
ESO 122-016 (SW) [P1]	96/11	1200	9780					non-ac
MCG -01-22-27	98/03	1200	4575	7.03	1.16	21.86	7410	H II
NGC 2650	98/03	1200	4356		0.08		8610	Sy 1.8
MCG +08-17-60 (N)	98/03	1200	15950					non-ac
CGCG 037-023	98/03	1200	13158		0.29		410	H II
NGC 5098 (E)	98/03	600	10970					non-ac
VII Zw 608 (W)	97/08	1200	20640					non-ac
MCG +07-37-018 (SW)	97/08	900	14070	0.89	0.29			H II

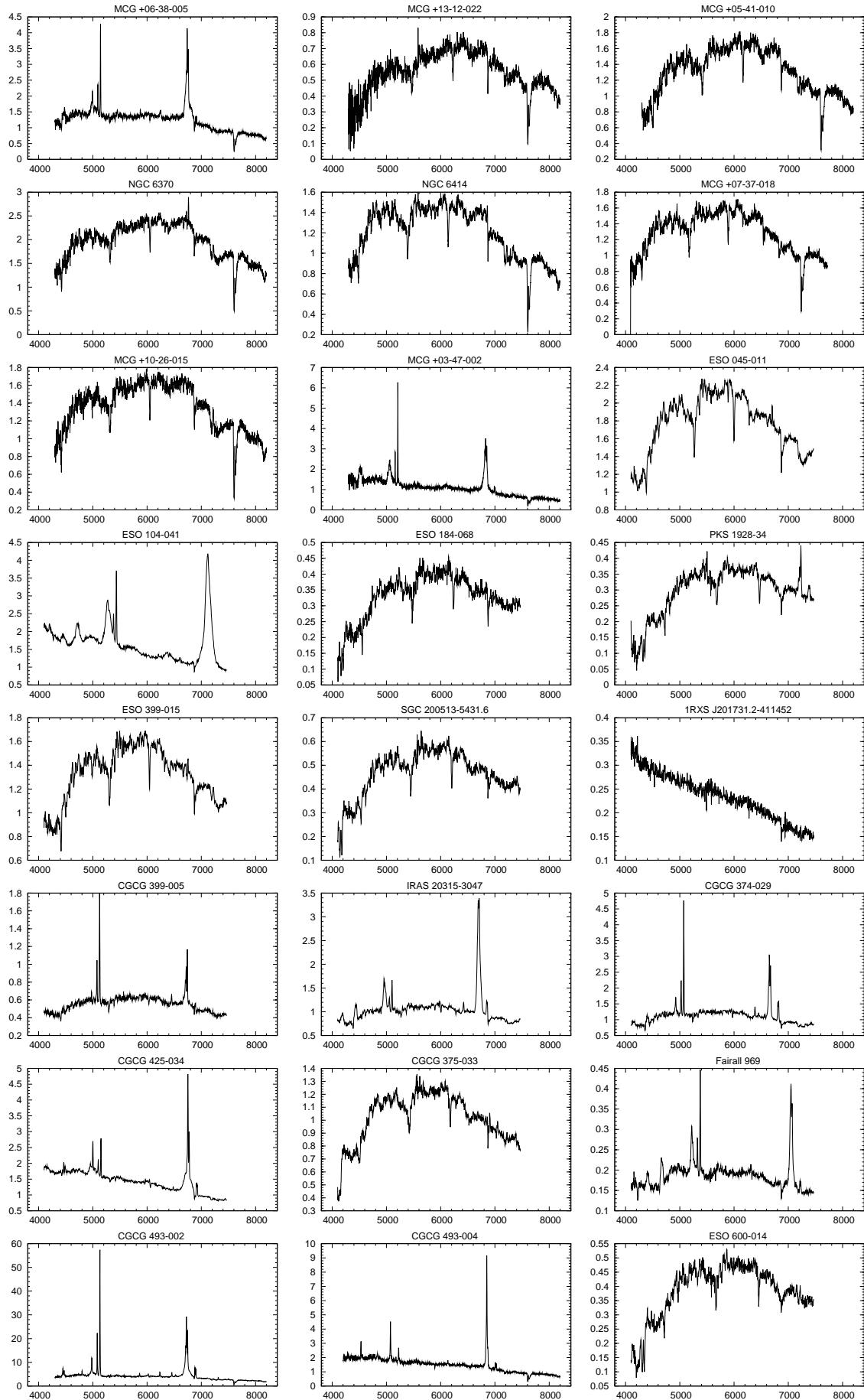
Main Targets:

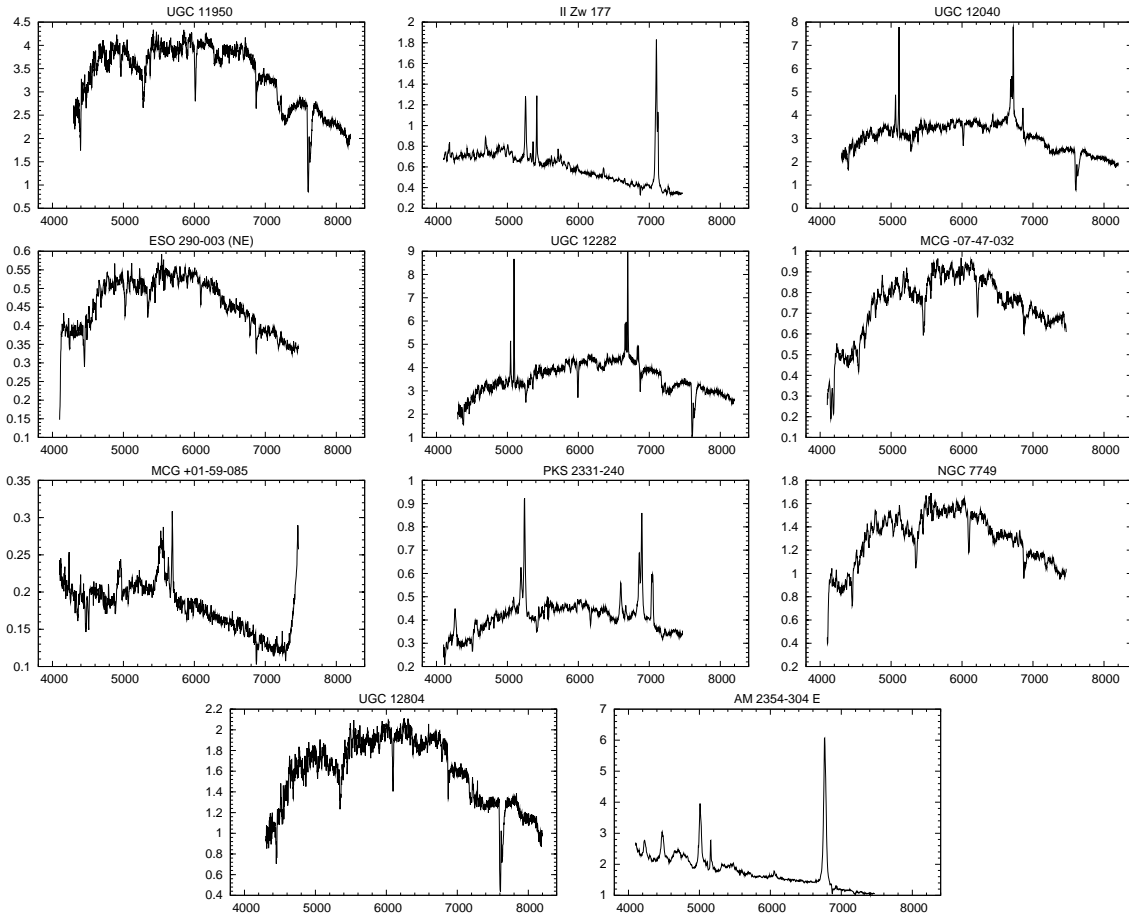












Companions:

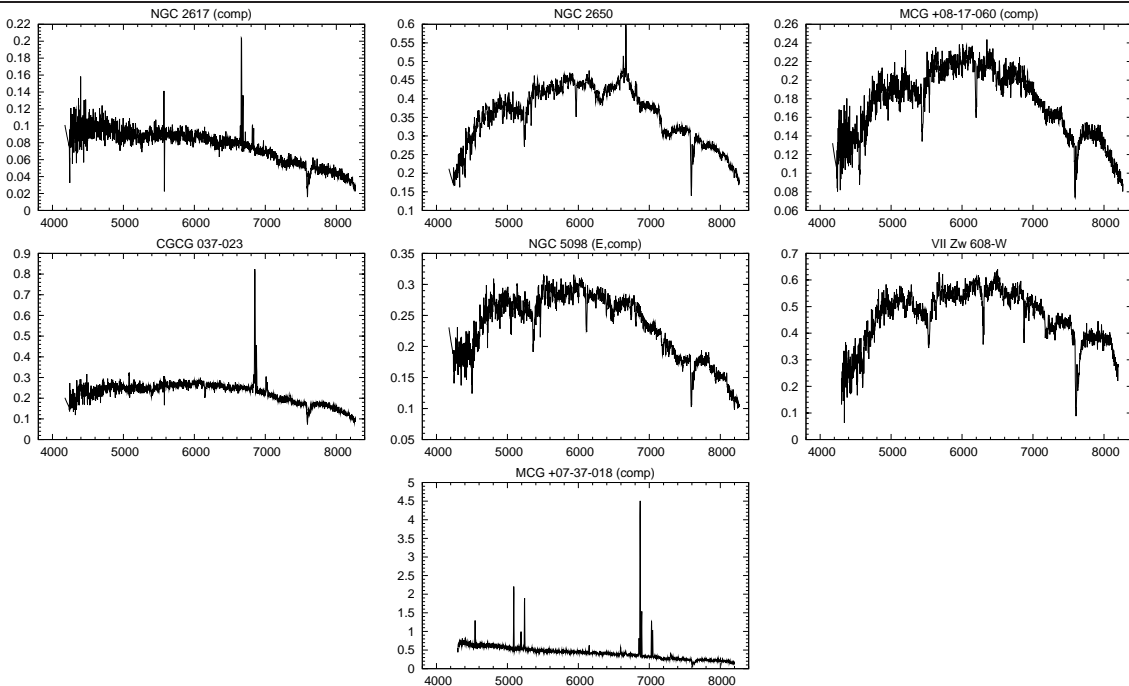


Fig. 11. Spectra of all objects of our sample